

Design and Testing of an Infrared Ice Detector System for Helicopter Blades

by

Marie-José Martinez

Ingénieur de l'École Polytechnique, 1995

Submitted to the Department of Aeronautics and Astronautics
in partial fulfillment of the requirements for the degree of

Master of Engineering in Aeronautics and Astronautics

at the

MASSACHUSETTS INSTITUTE OF TECHNOLOGY

May 1997

© Massachusetts Institute of Technology 1997. All rights reserved.

Author
Department of Aeronautics and Astronautics
May 9, 1997

Certified by
Charles Boppe
Senior Lecturer, Department of Aeronautics and Astronautics
Thesis Supervisor

Certified by
John Hansman
Professor, Department of Aeronautics and Astronautics
Thesis Supervisor

Accepted by
Jaime Peraire
Chairman, Department Graduate Committee

MASSACHUSETTS INSTITUTE
OF TECHNOLOGY

JUN 19 1997

ARCHIVES

LIBRARIES

Design and Testing of an Infrared Ice Detector System for Helicopter Blades

by

Marie-José Martinez

Ingénieur de l'École Polytechnique, 1995

Submitted to the Department of Aeronautics and Astronautics
on May 9, 1997, in partial fulfillment of the
requirements for the degree of
Master of Engineering in Aeronautics and Astronautics

Abstract

Passive infrared ice detection has recently been developed at Visidyne, Inc. in association with NASA Lewis Research Center and the US Army, as a new technology to detect ice accretion on rotor blades through the measurement of the latent heat radiated when ice builds up on the leading edge of the blade. This project is intended to be a contribution to the design effort conducted at Visidyne. First, market assessment studies analyze the worthiness of the new product, the potential market and the basic requirements stated by the possible customers. Then the experiments conducted with three different types of infrared detectors to validate the technology and select the best performing sensor, are described. After different series of experiments, the concept has proved efficient but before the actual prototype of the passive sensor is designed, some problems related to the low operating temperature have to be addressed. A practical design solution to prevent the optical system from icing, thus detecting nothing, is proposed in the last part of this report.

Thesis Supervisor: Charles Boppe

Title: Senior Lecturer, Department of Aeronautics and Astronautics

Thesis Supervisor: John Hansman

Title: Professor, Department of Aeronautics and Astronautics

Acknowledgments

The work presented here has benefited from many contributions and I would like to thank all the people that have made this project possible.

I am particularly grateful to the members of my "team" at Visidyne and at MIT for involving me in the project and providing help. Thanks to Ron Rieder for taking the time to support my work. Thanks to Sanjay Krishnaswamy for all the explanations. Special thanks to Prof. Hansman for his advice and enthusiasm. I learned a lot with him, and specially that I still have a lot to learn.

I would like to express my gratitude to Charlie Boppe for his time and continuous support. Thanks to Délégation Générale pour l'Armement for funding my academic year at MIT. I hope, in return, that they will get the benefits of the education I received here. I am particularly grateful to Mrs. Edith Roques, from Supaero, for all the time she devoted in helping me prepare this year at MIT.

I am gratefully indebted to all those that helped me writing this report and supported me all the time, Gael, Frédéric and specially David, for whom there are no words to express my gratefulness.

Contents

- 1 Introduction** **13**

- 2 Background** **15**

- 3 Market Assessment - Motivation for a remote ice accretion detector and derivation of requirements-** **19**
 - 3.1 Icing in helicopter flight 20
 - 3.1.1 Parameters of influence 20
 - 3.1.2 Ice prevention and elimination. The problem of blade icing 21
 - 3.1.3 Icing accidents 22
 - 3.2 Market studies 22
 - 3.2.1 Contacts 22
 - 3.2.2 Potential Market 24
 - 3.2.3 Possible customers 26
 - 3.2.4 Conclusion 27

- 4 Derivation of requirements** **29**
 - 4.1 Requirements for the detector 30
 - 4.2 Requirements for the Optics protection 32
 - 4.3 Conclusion 34

5 Experiments.	35
5.1 Experimental setup	36
5.2 Analysis of the results	37
5.2.1 Responsivity to the radiation from a blackbody.	37
5.2.2 Characteristic parameters of detectors. Detectivity, Noise Equivalent Power	38
5.2.3 Noise Equivalent Power. Noise Equivalent Temperature	39
5.3 Experimental results for the pyroelectric detector	40
5.3.1 Responsivity	40
5.4 Frequency Response	41
5.4.1 Field-of-View	42
5.5 Experimental results for the Lead Selenide Detector	44
5.5.1 Responsivity	44
5.5.2 Frequency Response	47
5.5.3 Field-of-View	48
5.6 Experimental results for the MCT detector	50
5.6.1 Responsivity	50
5.6.2 Field-of-View	51
5.7 Noise spectrum Analysis	52
5.8 Effects of heating a window	55
5.9 Field experiments	56
5.9.1 Experimental conditions	56
5.9.2 Analysis of the experiments	57
5.9.3 Pictures	58
6 Lens protection design considerations.	61
6.1 Background: relevance of a protecting subsystem, possible solutions.	61

6.2	The heated window option	62
6.2.1	Preliminary considerations	62
6.2.2	Noise considerations	63
6.2.3	Choice of materials	65
6.2.4	Choosing the heating device	75
6.3	The mirror option	77
7	Design integration and preferred concept	79
7.1	The gold grid protection	80
7.2	The bleed air concept	82
7.3	The heated mirror concept	82
7.4	Possible integration on the helicopter	83
7.5	Integration Cost	86
7.6	Comparison of Concepts	86
8	Conclusions and Recommendations	91
	APPENDICES	94
A	Chronology of the Project	95
B	Blackbody Radiation	97
C	Acronyms	99
D	Summary of Interviews	101
D.1	Organizations	102
D.1.1	Délégation Générale pour l'Armement	102
D.1.2	Federal Aviation Administration	102

D.2	Manufacturers	103
D.2.1	Eurocopter France	103
D.2.2	American Eurocopter	103
D.2.3	Sikorsky	104
D.2.4	McDonnell Douglas	105
D.2.5	Boeing	105
D.2.6	Bell Helicopters	105
D.3	Services	106
D.3.1	Era Services-Alaska	106
E	List of Contacts	107
E.1	On general topics related to helicopter icing	107
E.2	On market possibilities	107
E.3	On the protective device	108
F	Experimental Investigation of Passive Infrared Ice Detection for Helicopter Applications	109

List of Figures

2-1	Schematic Representation of Latent Heat Release During Icing	15
2-2	Typical Temperature Signature for Simulated Conditions (with a spray of fake ice)	16
4-1	QFD Requirements Matrix for the Detector	31
4-2	QFD Requirements Matrix for Optics Protection	33
5-1	Experimental Setup	36
5-2	Frequency Response of the Pyroelectric Detector	42
5-3	Field-of-View of the Pyroelectric Detector	43
5-4	Field-of-View of the Pyroelectric Detector, Top View	43
5-5	Responsivity of the Lead Selenide detector	47
5-6	Detectivity of the Lead Selenide Detector	48
5-7	Field of View of the Lead Selenide Detector	49
5-8	Field of View of the Lead Selenide Detector, Top View	49
5-9	Field of View of the MCT Detector	51
5-10	Field of View of the MCT Detector, Top View	52
5-11	Noise Spectrum of the Pyroelectric Detector	53
5-12	Noise Spectrum of the Lead Selenide Detector	53
5-13	Noise Spectrum of the Mercury Cadmium Telluride Detector	54
5-14	Detectivity of the Lead Selenide Detector Determined from Noise Spectrum Data	55

5-15	Field Test Setup	57
5-16	View of the R22 Helicopter used for the Field Experiments	58
5-17	View of the Detectors Mounted on the Helicopter	59
5-18	Close-up View of the Detectors	59
5-19	Example of Blade Icing (1)	60
5-20	Example of Blade Icing (2)	60
6-1	Comparison of the properties of different materials for infrared windows	67
6-2	Spectral Window (left) and Refractive Index (right) for Different IR Materials . .	68
6-3	Coefficient of Thermal Expansion (left) and Surface Hardness (right) for Different IR Materials	69
6-4	Young's Modulus and Rupture Modulus for Different IR Materials	70
6-5	Transmittance of CVD ZnS 6 mm Thick, Multispectral Curve (top); Transmittance of CVD ZnSe 10 mm Thick (bottom)	74
6-6	Sketch Of The Mirror System Implementation	77
7-1	Gold grid heated window concept	81
7-2	Bleed Air Concept	82
7-3	Mirror Concept	83
7-4	Exploded View of Eurocopter Super Puma	85
7-5	Comparison Matrix	88
7-6	Concept Ranking	89
A-1	Chronology of the Project	95
B-1	Typical Blackbody Radiation Curves at Different Temperatures	97

List of Tables

5.1	Experimental Results for Responsivity Determination-Pyroelectric detector . . .	41
5.2	Experimental Results for Responsivity Determination-Lead Sellenide Detector . .	45
5.3	Figures of Merit of the Lead Sellenide Detector	46
5.4	Experimental Results for Responsivity Determination-MCT detector	50
6.1	Percentage of DC Signal Added to Each Detector by a Heated Window	64
6.2	Comparison of the transmittance for GaAs and Germanium windows as a function of flight time	72

Chapter 1

Introduction

Information about ice accretion on rotors is of significant importance to flight safety in all-weather operation since blade icing results in severe performance and control degradation. To date, most ice detector systems used in aviation applications are based on contact type devices. Though efficient to detect ice accretion in the airframes, these systems cannot be implemented in rotor blades for different practical reasons including structural limitations of the blade, acceleration limitations of the sensors, difficulty transmitting information between the rotating and non rotating parts, and erosion. Therefore, information on ice buildup on rotating surfaces used to be inferred from ice conditions on the fuselage, which appears faulty because icing conditions on the fuselage and on the rotating blades may be substantially different.

To detect ice accretion on the blades, a method based on the remote detection of the latent heat released by the solidification of water has been studied at MIT and applied at Visidyne, a company specialized in optical systems. As a result, the prototype for an infrared ice detector has been designed. Three different infrared sensors have been proposed: a Mercury Cadmium Telluride, a Lead Selenide and a Pyroelectric detector. Their performance is significantly different, as is their cost. The selection of the preferred sensor is based on trade-offs, evaluated through a series of experiments that are described in the second part of this report. But this technical analysis says nothing about the value of such a detector. So the real question before any system is designed, should be : is this product useful ? If icing is undoubtedly a critical problem in helicopter flight, the worthiness of a detector for blade icing is based on two main

considerations. One is related to the significance of blade icing versus airframe icing. The other addresses the importance of having an ice detector equipped aircraft. This is discussed in the first part of the report along with the requirements that possible customers would expect from the product.

It appears that both the derived requirements and the field experiments show the need to have an all-weather, and hence ice-protected detector. This all-weather issue, crucial for the performance of the detector is analyzed in the last chapters. To protect the optics from icing, several design solutions are examined and compared.

Chapter 2

Background

The development of a remote ice detector for rotor blades is a joint venture between MIT and Visidyne, Inc. This was initiated at MIT, by the research work of Pf. Hansman and A. Dershowitz, on the feasibility of this new kind of ice detection (see [1], [2]). A copy of the paper presenting this research is included in Appendix F.

Remote ice detection is based on the measurement of the latent heat released by supercooled water droplets as they turn to ice on the leading edge of the blade. A schematic representation of this idea is the following¹:

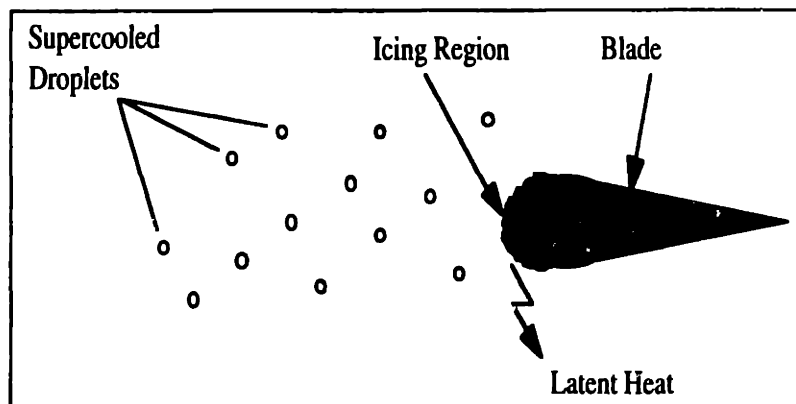


Figure 2-1: Schematic Representation of Latent Heat Release During Icing

¹From [2].

To detect this heat, an infrared detector is used as a thermometer that measures the temperature of the blade along the chord, based on the blackbody radiation emitted from the blade. As a result, a temperature profile of the blade can be mapped chordwise. When no ice has built up, the temperature signature across the blade is flat: the radiation from the blade is roughly uniform chordwise, whereas when there is ice on the blade, a characteristic peak temperature (of a few degrees Kelvin) appears around the leading edge, because this is the place where ice builds up and heat is released. Typical temperature profiles are shown in the following figure obtained in lab simulated conditions (from [1]).

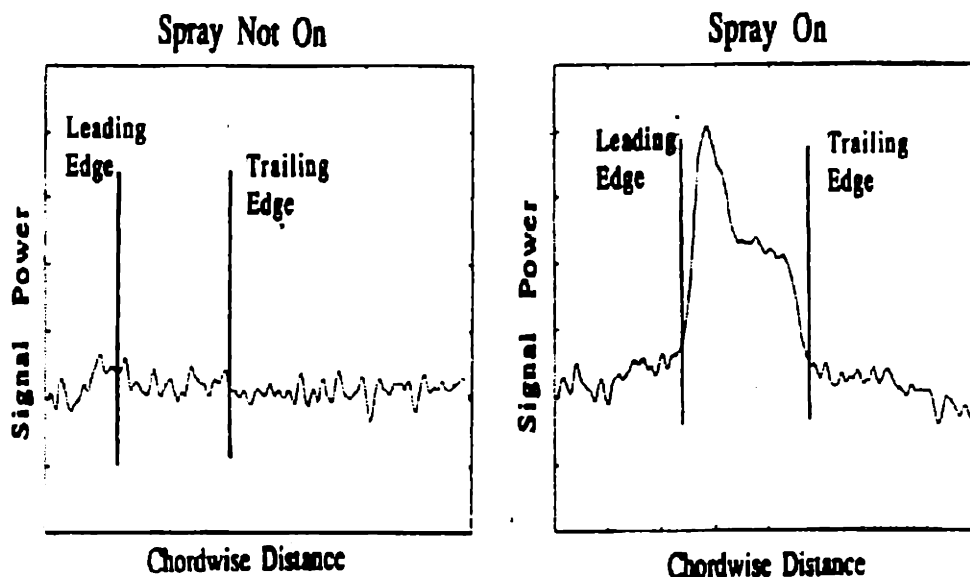


Figure 2-2: Typical Temperature Signature for Simulated Conditions (with a spray of fake ice)

On the first plot, no artificial snow was sprayed and the temperature profile from the leading edge to the trailing edge is flat. On the second plot, the snow source was on and a characteristic peak appears close to the leading edge². Note that the infrared thermometers (detectors) considered are AC coupled, so that they are sensitive to temperature variations only.

In 1996, Visidyne, Inc. was funded by NASA for a two-year program to implement the idea of a remote ice detection system (phase 1) and eventually design the prototype (phase 2). Several series of field experiments were conducted to evaluate the validity of the theory. The first series did not yield results essentially because of the failure of the data acquisition system. The last

²This is discussed in [1], [2]

series were conducted this winter with an improved experimental setup and data acquisition system. They were intended both to check that an icing signature was observable, and to compare the performance of three types of infrared detectors. At this point, the feedback obtained from the field experiments and the contacts with the customers, NASA and the Army, has been implemented in the design of the prototype, that should be tested in the winter of 1998.

Chapter 3

Market Assessment - Motivation for a remote ice accretion detector and derivation of requirements-

The analysis of the potential market for a remote ice detector has been established with the use of several metrics of worthiness that include safety and operations. This means that the value of the detector was derived from the answer to the following questions :

- How critical is blade icing for safety ?
- How important can it be to operational activities ?

These questions actually address two kinds of issues. One is related to the value of an ice detector, the other to the specific value of a remote detector, or a detector for blade icing. Several contact-type devices have been developed to detect ice on airframes, but a remote detector would be the first and only product of this kind in the market. This can be an asset provided there is a specific need for it and the detector's efficiency is proved. The objective of this chapter is to discuss more particularly the first condition, whereas the latter will be analyzed in subsequent chapters.

3.1 Icing in helicopter flight

3.1.1 Parameters of influence

There is no complete theory to date to model icing. The complexity of the process and the number of parameters it involves are such that it cannot be fully forecasted. One of the main difficulties lies in simulating surface accretion. Yet, some weather conditions are known to be favourable and some parts of the aircraft, such as engine inlets or thin profiles, seem more sensitive to icing. Important parameters to predict ice occurrence include:

- *the shape of the part considered and its speed.* Near the tip of a blade for example, the air is compressed and warms up, which limits the accretion. However there is no clear understanding of how the shape of the profile is correlated to the formation of ice. On a helicopter for example, the blades seem to be sensitive to icing but there is no evidence that they will ice up before or after the airframe.
- *the temperature and the atmospheric content of liquid water.* The presence of liquid droplets in the air, whether visible (precipitations) or invisible, is a necessary condition for icing. Below -20°C it is hard to find liquid, the water has turned into ice crystals and therefore icing is rare: less than 4 % of icing happens at temperatures lower than -20°C whereas most of the icing occurs when temperature ranges between -15°C and 0°C .
- *the size of the water droplets.*

These parameters also determine the type of icing: rime ice or clear ice . The former is the more frequent (75–80% of the cases). It builds up on the forward edges, without really changing the shape of the profile. Most of the deicing devices are concentrated on the removal of this kind of ice. The latter is more critical and harder to see. It appears at warmer temperatures (typically above -10°C but not always), for higher water contents and larger drops. It results in an uneven air flow down the profile that spoils the performance. It can be removed by sublimation or by melting.

3.1.2 Ice prevention and elimination. The problem of blade icing

The risk of encountering icing conditions in flight is advised to pilots through weather forecasts before take-off. According to this information and the kind of helicopter used, the pilot can decide to cancel the flight or proceed with possible limitations. The problem is that meteorological conditions can vary quickly with time constants of the order of one to two hours even minutes in the case of fast moving cold fronts. Therefore there is a probability that icing conditions are met unexpectedly, in which case, there are different scenarios that depend on the equipment of the aircraft.

If the helicopter is equipped with ice detectors, the pilot will get information well in advance to adopt a strategy to escape icing conditions. This includes climbing above the clouds to sublimate the ice, staying at the same level but flying towards the warm air, trying to land or if applicable, using deicing devices. Ice can then be removed in a few minutes down to a few seconds if deicing capability is used. In any case, since there exists no detector to give information on blade icing, the pilot has to infer what is happening on the blades from the airframe detectors and temperature sensors. Moreover, when the helicopter is equipped with electro-thermal deicing devices for the blades, the lack of detection capability results in their inefficient use, and therefore inadequate waste of power, that could be necessary in critical flight maneuvers.

When the aircraft has no ice detectors, there is a risk that icing will be noticed from its consequences. If icing occurs in the carburetor, it will manifest itself by a loss in engine power. If it occurs on the blades, abnormal torque rise will be noticed and vibrations, due to uneven shedding of the ice, will follow quickly. How critical this is depends on the size and shape of the blades. Longer thicker blades can resist icing more easily. In some cases, the pilot will barely notice the effects of the ice and degradation of performance can appear after thirty minutes. For thinner blades with a smaller chord, the accretion efficiency is higher and vibrations will be noticed after a couple of minutes only. The margin of maneuver can then be very limited, if any, because quick actions might not be possible any longer at this point, especially if the helicopter is not powerful enough.

3.1.3 Icing accidents

Icing has proved to be a significant cause of accidents or incidents in aviation statistics. Briefs from the National Transportation and Safety Board (NTSB)¹ show that over the past 14 years in the United States, 25 helicopter accidents involved icing. In almost 80% of the cases, carburetor icing conditions and ice in the fuel system were encountered. Icing of the induction air control system or the primary servo of the rotorcraft flight control system was also suspected in two accidents. Though the responsibility of the pilot was proven in several accidents for flying under known adverse conditions, which includes poor preparation of the flight, the failure in most of the cases to properly use carburetor heat and/or de-icing devices reveals that the pilot “unexpectedly” encountered icing conditions in flight and reacted after suffering the consequences of icing, evidenced by a loss of engine power.

Even if there is no explicit record of accidents caused by blade icing, all reports of flight incidents under icing conditions indicate that:

- it is not straightforward to predict icing occurrence even if some weather conditions are favorable,
- evidence of icing is often derived from the degradation of helicopter performance, which can be very rapid and dramatic².

Consequently ice detection capable systems appear worthwhile if not critical for certain applications.

3.2 Market studies

3.2.1 Contacts

The market studies presented in the following sections are based on interviews with helicopter manufacturers, services and governmental organizations in the United States, France and Russia.

¹See [13]

²A revealing example was provided by a pilot from the French Armed Forces who reportedly lost 6,000 ft. in 90 seconds when he faced icing conditions in flight (reported by M. Corlay from DGA).

The contacts included ³:

- *Manufacturers*

- Eurocopter France, American Eurocopter
- Sikorsky
- McDonnell Douglas
- Boeing
- Bell Helicopters
- Robinson and Augusta

- *Services*

- Era Services, Alaska

- *Organizations*

- NASA Lewis Research Center
- US Army
- National Center for Atmospheric Research
- National Transportation Safety Board, Federal Aviation Administration
- Délégation Générale pour l'Armement (France)
- State Scientific Research Institute of Civil Aviation (Russia)

Even though not all the contacts listed could actually provide support for the study, the information collected made it possible to get some insight on the position of the proposed detector on the existing market, the needs in terms of ice detection, the market for the detector and the requirements of potential customers.

³For further details, see appendix D.

3.2.2 Potential Market

Normally, helicopters that are not certified to fly under icing conditions should not take off when there is a risk of encountering these conditions. The previous analysis shows that this is not always an obvious decision. Moreover, some activities require almost "all-weather" operations without necessarily having adequate all-weather aircraft. This section is intended to evaluate which helicopters would get the most benefit from having an ice detector for the blades.

The problem with certification/qualification

It appeared very soon in these market studies that targetting icing certified helicopters, that are required to have ice detection and protection capability, would not be a good strategy because there is only one kind of helicopter certified to fly under "unlimited" icing conditions⁴: Eurocopter Super Puma, first model. The cost of certification is so high that neither manufacturers, nor operators are willing to make the investment for a market that seems narrow anyway as revealed by the limited number of Super Puma sales and the lack of other candidates for certification⁵ except for Russian helicopters such as MI-8/32. Certifying the Super Puma costed about 300 million French francs⁶. Different factors account for such dramatic costs. The difficulty to completely model ice accretion and its consequences makes it necessary to use flight evaluations to study accretion efficiency (of ice), mechanical resistance, aerodynamic consequences of profile deformation and consequences of ice shedding. Regulations⁷ require around 60 flight hours under specific icing conditions for certification. But in fact, about 50 % of the flight time is really efficient in terms of appropriate weather conditions. This results in long certification processes (200 flight hours were necessary to certify the Super Puma⁸), that can take years.

It is interesting to note at this point, that not all the countries have such stringent rules for

⁴Except Russian helicopters maybe, but little information is available for them.

⁵Super Puma model 2 might be certified eventually, though the process was delayed due to the cost. Sikorsky SH-76 was close to being certified, but again the cost of the process and the modifications were deterrent.

⁶Around 50 million dollars.

⁷These are the French rules imposed by the Direction Générale de l'Aviation Civile, they are close to US FAA rules.

⁸One flight hour costs about 10,000 Francs or 2,000 US dollars, I leave the calculations to the reader...

icing certification. Great Britain allows certification for light icing conditions, provided the pilot flies at a minimum altitude of 500 ft. above the sea level⁹ and can take advantage of the favorable temperature gradient existing above the sea to descend and escape icing. Other countries that have limited icing conditions certification include the Netherlands and Turkey.

Another alternative to certification is qualification. In that case, the helicopter is qualified to an extended flight envelope not as stringent as for certification, for use by the Military. This is the case of Sikorsky's Blackhawk sold to the Army and Navy with electrothermal heating devices along the blades. Eurocopter NH90, helicopter for European armies should also be icing qualified.

This analysis shows that the primary market for the detector extends beyond the domain of icing certified helicopters. Qualified helicopters might be a better target, but also, as will be shown in the next subsection, civilian IFR¹⁰ certified helicopters, could be a large market, specially for some specific operations.

An advisory system for medium size helicopters

Icing, especially on the blades, appears as a more critical issue for small/medium size helicopters. In fact, smaller size helicopters are usually VFR certified and consequently, the risk that they encounter icing conditions for the blades¹¹ is smaller if the pilot respects the rules. Indeed, this kind of helicopter should not fly in the clouds, where the probability of icing is higher. In any case, if a VFR helicopter were submitted to icing, the conditions would probably be such that the major problem would be navigation (visibility) and not exclusively icing.

For IFR, medium size helicopters, the problem is different. They are often used for bad-weather operation, without any icing certification. As a basis, all aircraft have engine inlet protections and must demonstrate an acceptable visibility through the windshield. Some of them are equipped with airframe type ice detectors and temperature sensors on the windshield and could possibly take advantage of a blade ice detector, specially if the size of their blades is

⁹This rule was actually adopted for operations in the North Sea.

¹⁰Instrument Flight Rules : this certification allows to fly without visibility (in the clouds) provided there is minimum equipment on board. On the contrary, VFR, Visual Flight Rules, do not allow flight with no visibility.

¹¹Icing conditions for the carburetor are more common.

critical in terms of icing as described in the previous sections. Eurocopter is conducting some research for icing on medium size helicopters such as the Ecureuil and the Dauphin, used for emergency evacuation. In this case, the detector would be valuable as an advisory system, that would give information to the pilot soon enough to take the adequate action. Even if this would not permit flight in known icing conditions it would contribute to improving safety for situations where icing is encountered in flight. This is particularly crucial for some operations that require large availability.

3.2.3 Possible customers

Many operators seem interested in having all-weather certified helicopters. The problem is that, regarding icing, the costs of certification are so high that few operators are willing to invest, specially if certification affects a reduced part of their fleet. Consequently, ice detection capability becomes an asset for medium-size helicopters used by:

- *Commercial Transport.* This might be a reduced market localized to cold northern regions such as Canada, etc. Sikorsky's EH-101 /S92 have the largest market for commercial transportation and industrial utility.
- *Corporate executives.* Though this is not a large market, (Richard Fleming at Sikorsky helicopters estimates that this represents one or two helicopters per year), it has very high requirements in terms of availability. (Donald Trump, for example, has a Super Puma.)
- *Emergency/Medical Evacuation.* In this case, flight delays or cancellations are often unacceptable, which raises the dilemma of emergency vs. safety. That is why Eurocopter is working on the protection of helicopters used for medical evacuation.
- *Off-Shore Operators.* Era services in Alaska reported that oil companies amounted to 60% of their operations, for which icing was the most critical. In the North Sea, off-shore operators have a high need for protected helicopters which results in the wide use of Super Pumas icing certified or light ice certified helicopters¹².

¹²Accepted by Great Britain and the Netherlands.

- *the Military.* This is possibly the largest market. High needs in terms of all-weather operations, along with less stringent rules for qualification provide a favorable field for the implementation of an ice detector. The number of sales of the Blackhawk¹³ reached more than 1500 for the US Military, let alone the military sales to Japan and Australia. The Navy and Marine corps also have about 200 Super Stallion, a good candidate for the detector. McDonnell Douglas also reported more than nine hundred sales of their AH-64D Apache to the Military¹⁴.

3.2.4 Conclusion

From the previous analysis, the existence of a market for the detector seems clear either as a necessary system for a certified helicopter, or, and this is more probable, as an advisory system for medium size helicopters, especially when blade icing is critical. According to the different manufacturers, implementation of the detector could be considered on the following helicopters:

- Eurocopter: Super Puma, Dauphin, Ecureuil, AS 350 Astar, NH 90
- Sikorsky : S76, S92, CH-53E Super Stallion, UH-60 Blackhawk, RAH-66 Commanche¹⁵
- McDonnell Douglas: AH-64D Apache, and MC 900 Explorer
- Boeing: V22 Osprey, CH-47D Chinook, RAH-66 Commanche
- Bell: Bell 212, Bell 412

provided they meet basic requirements in terms of size, weight, cost, and of course functionality. This is analyzed in the next chapters.

¹³Equipped with ice protection devices

¹⁴Figures for European Armies are much smaller, given their size. The French Army, for example, has about 24 Super Pumas.

¹⁵developed in association with Boeing.

Chapter 4

Derivation of requirements

The contract between NASA and Visidyne did not clearly specify a set of requirements for the detector, except for the functionality. Analysis of the customers' requirements is, however, an essential step before any prototype is designed. Interviews with manufacturers and the help of MIT faculty made it possible to establish the expectations and constraints for the detector. It appeared, from this study and the experiments on the detectors (described in subsequent chapters), that a protection subsystem for the optical system was needed. Therefore, the requirements for such a support subsystem have also been examined. In this chapter, the requirements are presented using a Quality Function Deployment Matrix approach.

The inputs for a QFD matrix are weighted customer needs. Top needs are given 10 and less important ones are given a relative weight of 1. For each need, a set of technical requirements is derived and listed as vertical inputs of the matrix. The way these technical requirements meet the initial customer needs is reflected through a number 1,3 or 9 (for the best match) that is multiplied by the original weight. The columns of the matrix are then added to yield a hierarchical list of technical requirements. In addition, the roof of the matrix shows possible conflicts between technical requirements.

4.1 Requirements for the detector

As for any aeronautical application, low weight, small size and low aerodynamic penalty have been listed by all the contacts as top requirements. Naturally, as for any product, low purchase cost and low direct operating cost appear as desired features. However, it seems that for this specific system, the difference will be made on how well it performs¹, so that the main requirements are actually related to high accuracy and high reliability. The resulting set of requirements is listed below, with their relative importance and the target values derived from information provided by MIT faculty.

- High Accuracy
 - fast response (10): a delay of about 10-15 seconds to detect ice accretion should be an objective so that the pilot gets the information on icing well ahead of sensing the vibrations (which appear after about 2 minutes in the worst case);
 - high detection performance (10) : the detector should be able to see ice build up down to 0.02 inches;
- High Reliability
 - low failure rate (9): this requirement relates to the occurrence of false alarms and the failure of the detector in flight. Both events should be minimized;
 - dispatch reliability (6): this means that the detector should be in running conditions as often as possible, but it does not seem to be a main priority;
- Low Aerodynamic/Stability Penalty (8): the way the detector is mounted on the helicopter should not induce significant drag penalties and its location on the helicopter should not introduce moment balance problems (this is particularly important in the tail boom);
- Low Power Requirements (8) : consumption of electrical power should be minimized;
- Low Weight (7) : about 2 to 5 pounds should be acceptable;

¹And this is all the more significant since the detector may be used as an advisory system as explained in the previous chapter.

- Low Purchase Price : a few thousand dollars should be a target unit price;
- Low Direct Operating Cost (7);
- Simple Operation (3) : this includes simple interface with the pilot;

Customer and technical requirements are combined in the following matrix².

QFD: Ice Detector

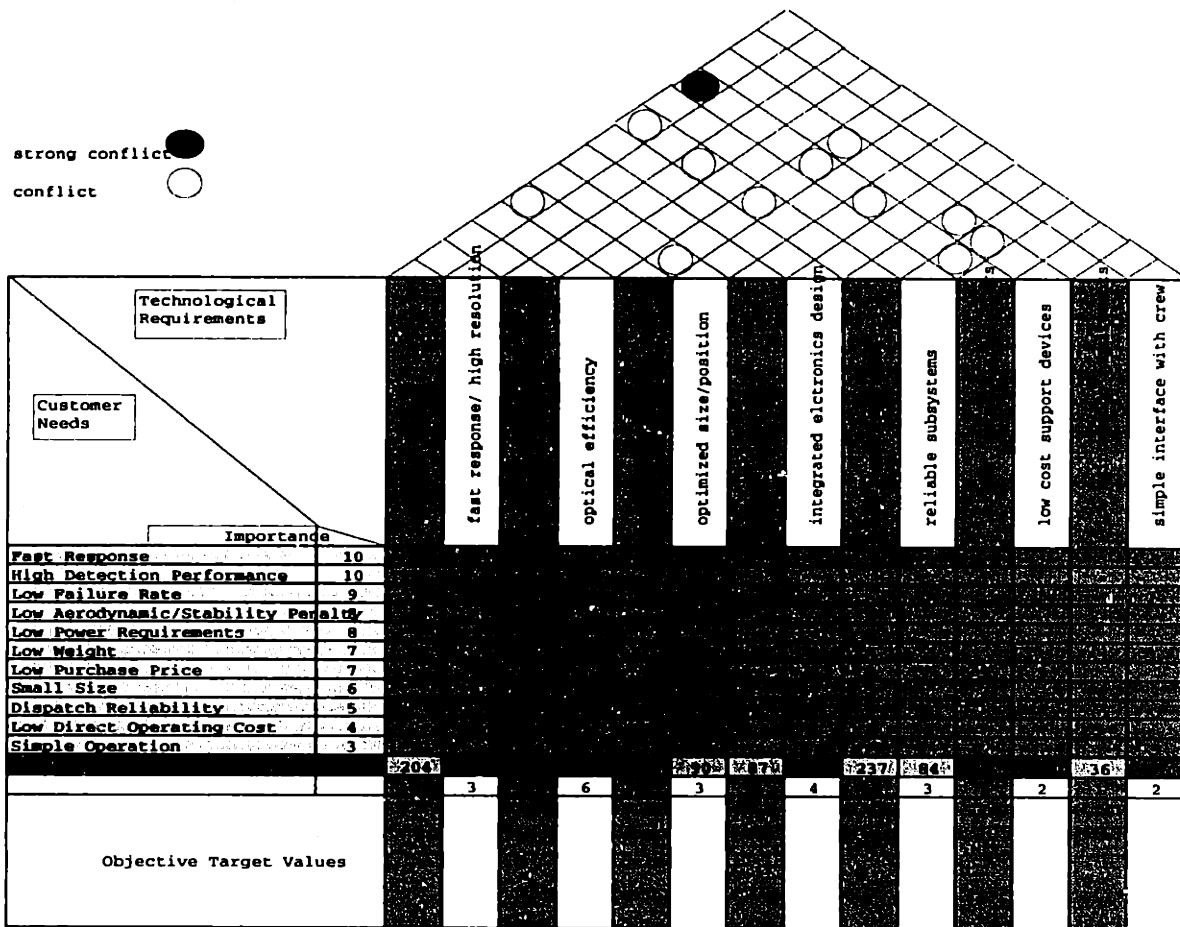


Figure 4-1: QFD Requirements Matrix for the Detector

This QFD requirements matrix leads to interesting results in terms of ranking the technical requirements. Few support devices for the system and high Signal-to-Noise ratio appear as

²The frame of this matrix is adapted from Matthew Burba's QFD developed for the MIT/Draper Technology Development Partnership Project.

top technical priorities. High Signal-to-Noise ratio was an expected technical target, because of the importance of accuracy and reliability. Few support devices was a less predictable top requirement. It actually relates to the number of devices needed by the detector, such as coolers/heaters, etc.

Attention should be paid to the fact that this matrix does not exactly include all the needs expressed by the customers, because some of them were demands for other systems. Indeed, de-icing capability and ice quantity determination capability were commonly expressed as desirable additional systems.

Moreover, it appears from the QFD matrix that protective devices for the optics are needed to ensure robustness to all-weather operation. Even if, with this set of weightings, this requirement seems secondary, field experiments, discussed in the next chapter show that this requirement is in fact critical for a low failure rate demand.

4.2 Requirements for the Optics protection

The purpose of the protection considered here is to prevent the lens of the detector from icing up under severe weather conditions. Therefore this subsystem supports the detector's operation, which implies that the constraints in terms of performance and interfaces are significant. The requirements for the protection are listed below with a coefficient of relative importance.

- No ice build up under severe icing conditions (10);
- Low interference with detector operation (9): this is related to a low noise penalty level and a high transparency in the infrared spectrum;
- High reliability (8);
- Low Power Requirements (7);
- Cheap relative to detector price (4): the price of the detector is a couple of hundred dollars³, the protective device should not add a significant cost of the whole system.

³Depending on the choice of the detector.

Consequently, the following Quality Dunction Deployment Matrix was derived:

QFD: Optics De-Icing System

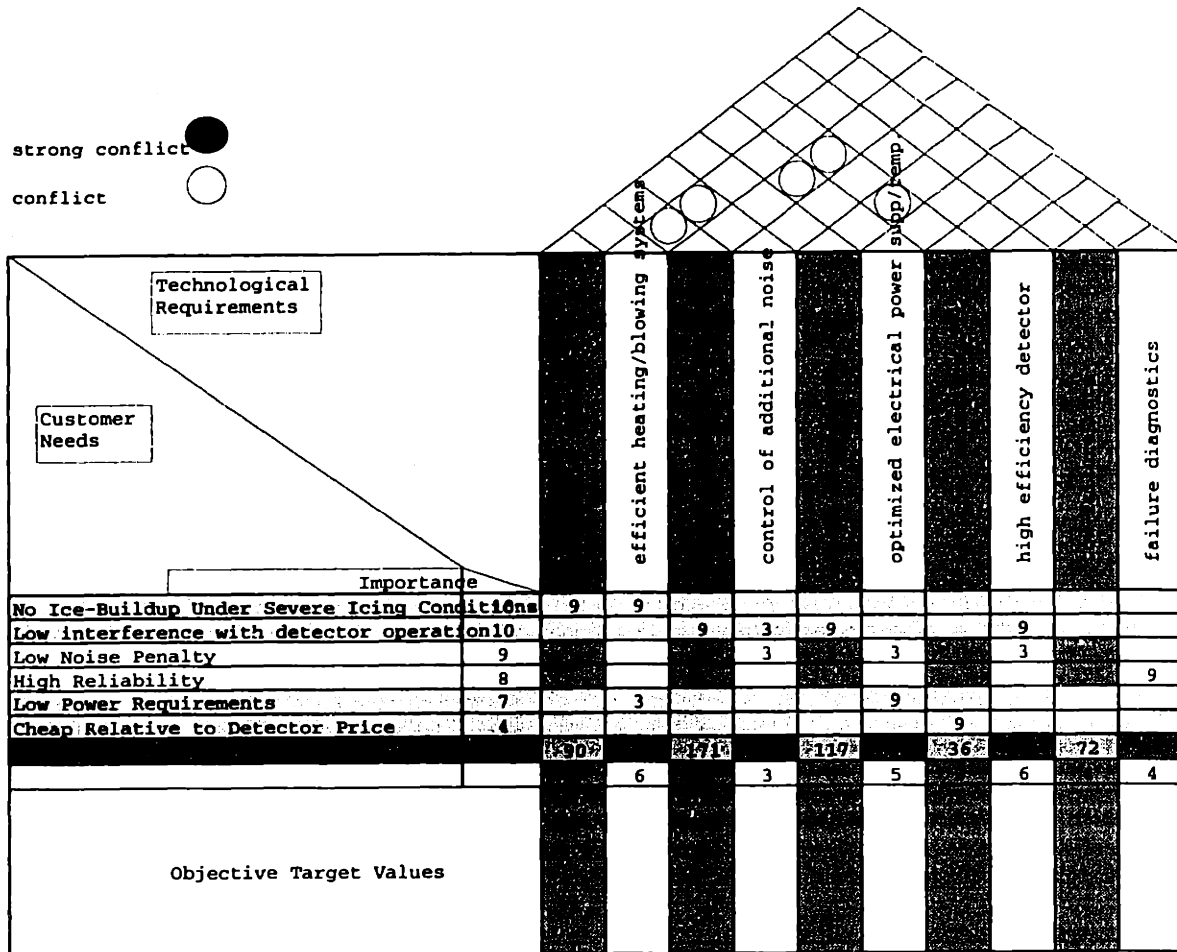


Figure 4-2: QFD Requirements Matrix for Optics Protection

In this case, top technical requirements are: low radiation versus signal, high transparency in the infrared spectrum, efficient heating/blowing system and high efficiency detector, which does not appear surprising. Note that no strong conflict has been identified at this point.

4.3 Conclusion

As obvious as it may be, the derivation of requirements revealed that establishing priorities among the initial needs expressed by the customers is difficult because everything appears important. The choice has then to be made considering the requirements from a different perspective, that is, examining the loss resulting from not addressing one of the requirements.

In addition, the way the QFD matrix is built may seem arbitrary, especially in the choice of the weighting factors. Indeed, modification of these factors leads to different prioritizations of the technical requirements. However, the “arbitrary” part of this choice is reduced by a team effort and possible iterations on the derivation of the matrix.

Chapter 5

Experiments.

To determine the feasibility of remote ice accretion detection, different series of field experiments have been carried out. The last one, described in the second part of this chapter, has been prepared by laboratory tests on three infrared detectors, Mercure Cadmium Telluride, Lead Selenide, and Pyroelectric, to derive their characteristics in terms of:

- Responsivity and/or detectivity, D^* ¹
- Frequency response
- Field-of-view

First, the results of this series of experiments make it possible to check that the detectors are operating properly according to the specifications provided by the suppliers, *CalSensors*, *Barnes Engineering* and *EG & G Judson*. Then, the characterization thus obtained serves as a basis to predict the behavior of the detector at low temperatures and to evaluate the conditions required for the detector to be efficient in detecting ice accretion. In the first part of this chapter, the experiments for this characterization are described and the results analyzed.

¹These terms will be explained in further detail later.

5.1 Experimental setup

In order to characterize the detectors, a blackbody is used at a temperature chosen according to the specifications of the detector. The utilization of a blackbody is preferred to a laser because the radiation occurs over a larger spectrum (in terms of wavelength)². This blackbody is located at the focal point of a parabolic mirror that collimates the beam on to the detector. The detector, used in association with a series of preamplifiers, is connected to an oscilloscope that displays the signal received. In addition, a chopper is included to set the frequency of the incoming beam. The basic experimental setup is shown in the following figure.

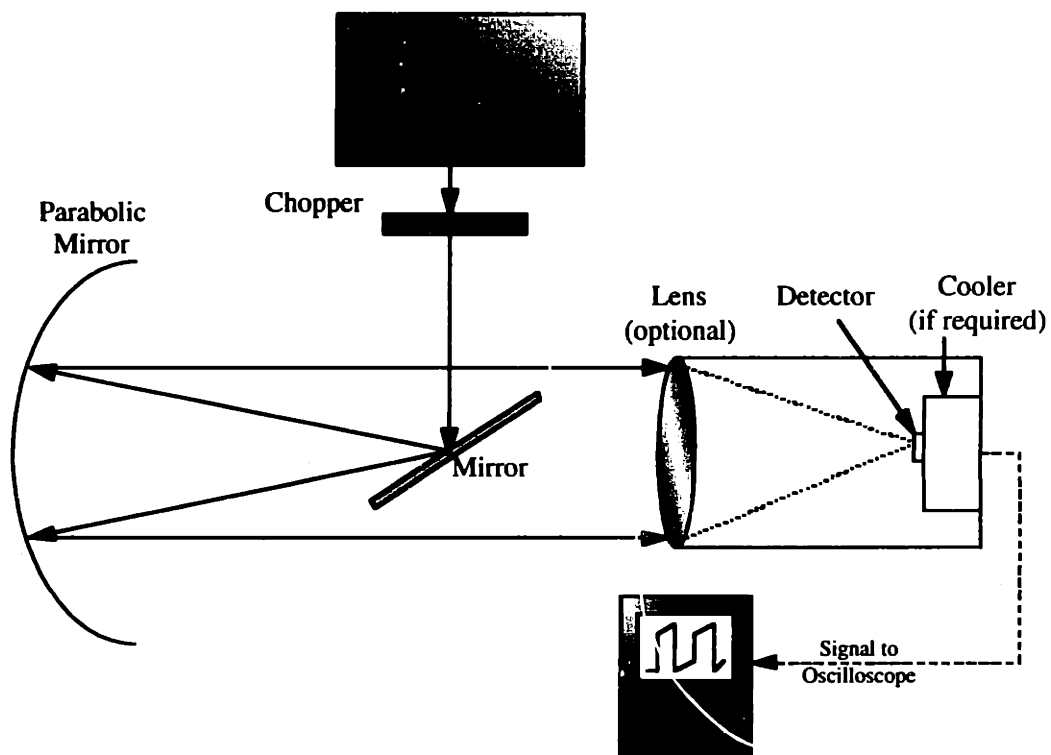


Figure 5-1: Experimental Setup

²See Appendix B for characteristics of radiation.

5.2 Analysis of the results

5.2.1 Responsivity to the radiation from a blackbody.

The responsivity of the detector is determined by the ratio of the output voltage (or current) to the input flux (in Watts). The output voltage is measured with the oscilloscope whereas the input power to the detector has to be calculated by applying the radiation laws according to the experimental conditions.

The spectral radiance (radiation per unit area, steradian, wavelength), emitted by a blackbody at the absolute temperature T , at wavelength λ , is given by Planck's law:

$$W_{\lambda}(T) = \frac{2c^2h}{\lambda^5 \left(\exp\left(\frac{hc}{\lambda kT}\right) - 1 \right)} \quad (\text{in } Wm^{-2}m^{-1}) \quad (5.1)$$

where c is the speed of light, h is Planck's constant, and k is Boltzmann's constant.

The total power falling onto the detector is then obtained by integrating the spectral radiance over the wavelength, λ , the area of emission, A , and the solid angle, Ω .

$$W(T) = \iiint W_{\lambda}(T) d\lambda d\Omega dA \quad (5.2)$$

The area over which the blackbody radiates is, in this case, fixed by the aperture, which varies between 0.0125 and 1 inch. The solid angle can be estimated by assuming that, since the beam from the mirror is collimated, the detector can be positioned at any distance from the mirror. Therefore if the detector were located very close to the mirror, the total solid angle would be:

$$\Omega = \frac{A_{\text{detector}}}{f^2}$$

where A_{detector} is the area of the detector cell and f is the focal length of the mirror. Note that if the detector is used in association with the focusing lens, the area of the detector is replaced by the area of the lens in the previous equation. By considering that the spectral radiance is constant over the solid angle and the area of emission, equation 5.2 reduces to a simple integral

whose limits depend on the spectral transmission of the detector. Actually, the detector acts like a filter over the wavelength. The shape of this filter depends on the detector characteristics chosen by the supplier. Here, it is assumed to be a square box, whose limits are:

- 3 to 5 μm for PbSe,
- 7.5 to 9.5 μm for HgCdTe, 4th. stage
- 3 to 17 μm for the pyroelectric detector.

Again, when a lens is used with the detector, an additional filtering should be accounted for by means of a factor of transmission, T (usually 80%), and a spectral transmission, that is also assumed to be a square box between 3 and 17 μm for the Germanium lens, and 0.15 and 7 μm for the Calcium Fluoride lens.

In fact, the signal received by the oscilloscope is related to the difference between the power emitted by the blackbody and the power emitted by the background (chopper blades in this case), considered as a blackbody at room temperature (298°K). The responsivity is consequently given by:

$$Responsivity = \frac{Signal}{W(T) - W(298)} \quad (5.3)$$

where *Signal* refers to the signal from the detector, which is different from the signal measured by the oscilloscope, by a factor equal to the gain of the amplifiers.

The noise level can be detector limited or amplifier limited. In this case, the electronic noise is limiting, although many improvements have been made throughout the calibration experiments.

5.2.2 Characteristic parameters of detectors. Detectivity, Noise Equivalent Power

The detectivity is a characteristic figure that takes into account the noise level in the detector .

It is given by:

$$D(T, F_c) = \frac{S}{N} \frac{1}{W}$$

where W is the incident power per unit area, S the signal and N the noise. For many infrared detectors, the noise is proportional to the square root of the size of the cell and to the square root of the bandwidth of the system. Therefore a specific detectivity (D^*) is defined by:

$$D^*(T, f_c) = \frac{S}{N} \sqrt{\frac{f_{3dB}}{A_{detector}}} \quad (5.4)$$

with: f_{3dB} being the electronics bandwidth, and f_c the chopping (or modulation) frequency. In terms of responsivity, the detectivity can be expressed as:

$$D^*(T, f_c) = \frac{\text{Responsivity}}{N} \sqrt{A_{detector} f_{3dB}} \quad (\text{in cm Hz}^{1/2}/W) \quad (5.5)$$

Several comments can be made on this quantity:

- since the noise in the system is limited by the amplifiers, the bandwidth should be the bandwidth of the noise spectrum. As a first approximation, the bandwidth of the system can be used to determine the specific detectivity. Rigorously, this bandwidth is estimated by considering the resolution in the power spectral density estimate of the measured noise. Both methods are used in the following calculations;
- the specific detectivity is a function of the temperature (of the blackbody) and of the chopping frequency;
- the detectivity measured in lab conditions is significantly different from the values that can actually be expected in real conditions.

5.2.3 Noise Equivalent Power. Noise Equivalent Temperature

The noise equivalent power is a measure of the power for a Signal-to-Noise ratio equal to one. It relates to the specific detectivity as the inverse.

$$NEP = \frac{1}{D^*} \quad (5.6)$$

If we account for the transmission losses due to the lens and the field-of-view of the detector, the Noise Equivalent Power for this particular application becomes³:

$$NEP = \frac{2 F^2}{\sqrt{f_{3dB}}} s T_0 D^* \quad (5.7)$$

where s is the size of the detector, and F represents the ratio of focal length-to-diameter for the lens.

Theoretically, this figure represents the minimum detectable power. In fact signals can be detected even if the Signal-to-Noise ratio is less than one, provided the noise is well defined and adequate filtering can be applied. Since the detector is intended to generate a temperature profile, the most important figure is the Noise Equivalent Temperature, which again corresponds to the standard deviation of the temperature or the temperature resolution that is given by:

$$\Delta T_{rms} = \frac{NEP}{\frac{\partial W(T,\lambda)}{\partial T}} \text{ in } ^\circ K \quad (5.8)$$

5.3 Experimental results for the pyroelectric detector

5.3.1 Responsivity

The responsivity has been evaluated with and without optics under the following conditions:

- Blackbody temperature: $1000^\circ K$ without optics and $500^\circ K$ with the optics
- Chopper frequency: 100 and 1000 Hz
- Area of the detector: $4mm^2$
- Heater temperature : $299^\circ K$ without optics and $300^\circ K$ with optics
- Gain of the amplifiers: 1364 at 100 Hz and 818 at 1000 Hz
- Noise level: $2 mV$ as a first approximation

³See [5]

In the calculations, the Germanium window associated to the detector has been accounted for in terms of transmission factor (80%) and spectral transmission (between $2.5\mu m$ and $14\mu m$). At $100Hz$ all three choppers have been used to make sure that no error is introduced by the use of one or the other chopper. The blackbody irradiance between 2.5 and $14\mu m$ is:

- at $500^{\circ}K$: $907.6W/m^2$ or $0.0908W/cm^2$
- at $1000^{\circ}K$: $14458W/m^2$ or $1.4458W/cm^2$

The corresponding power that gets to the detector is, at $1000^{\circ}K$, without window:

$$Power = \frac{0.09076}{\pi} Aperture(cm)^2 \frac{\pi}{4} \frac{Area_{detector}(cm^2)}{focal\ length\ of\ mirror\ (cm)}^2$$

The following table gives the results obtained for the responsivity, the detectivity and the Noise Equivalent Power assuming a system bandwidth of $600Hz$. Note that the real bandwidth is the noise bandwidth.

	frequency (Hz)	Responsivity (V/W)	Detectivity	NEP (W)
<i>without optics</i>	100	89.8	2.99e8	2.65e-6
	1000	26.2	5.25e7	18.7e-6
<i>with optics</i>	100	22.7	5.77e7	1.70e-5
	1000	11.8	1.70e7	5.75e-5
<i>values from supplier</i>	100	161	3.8e8	N/A
<i>irradiance is $4.28e - 4W/cm^2$</i>	1000	13	2.3e8	N/A

Table 5.1: Experimental Results for Responsivity Determination-Pyroelectric detector

5.4 Frequency Response

The frequency response was evaluated both with and without the optics at $773^{\circ}K$ and $500^{\circ}K$ respectively. Aperture of the blackbody was 0.2 inch for the first series and 0.1 inch for the second series. Because of the choice of the aperture in the first case, the results between the two choppers (fast and slow) are quite different. In both series of experiments, though, the results were rescaled to correct this error.

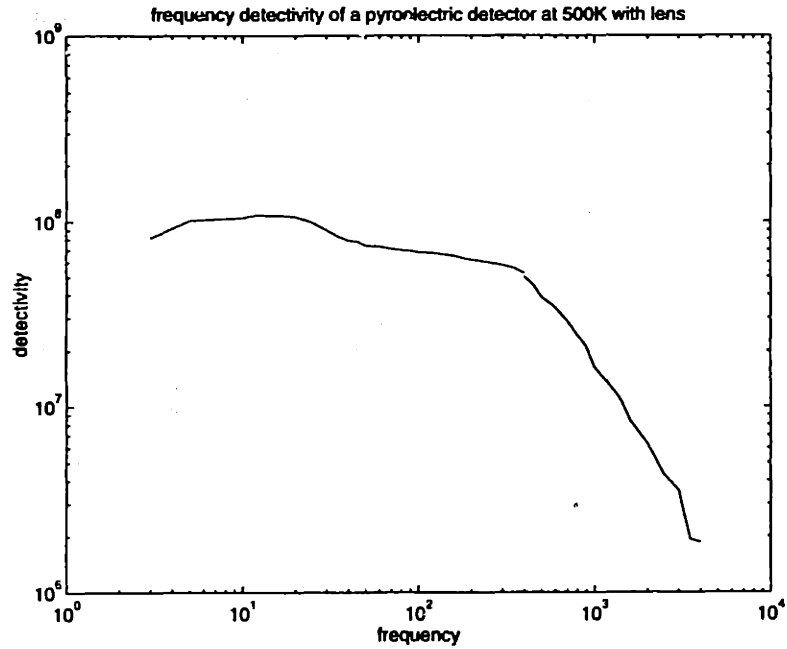


Figure 5-2: Frequency Response of the Pyroelectric Detector

5.4.1 Field-of-View

The field-of-view was determined using a 1000°K blackbody with a 0.05 inch aperture. No heating was used, so the temperature of the heater was 299°K. The field of view can be approximated by :

$$FOV = \frac{\text{size of detector}}{\text{focal length of lens}} = \frac{0.4}{10} = 0.04 \text{ rad} = 1.14 \text{ deg}$$

which is in good agreement with the experimental curves.

field of view for a pyroelectric detector, with a 0.05inch aperture blackbody at 1000K

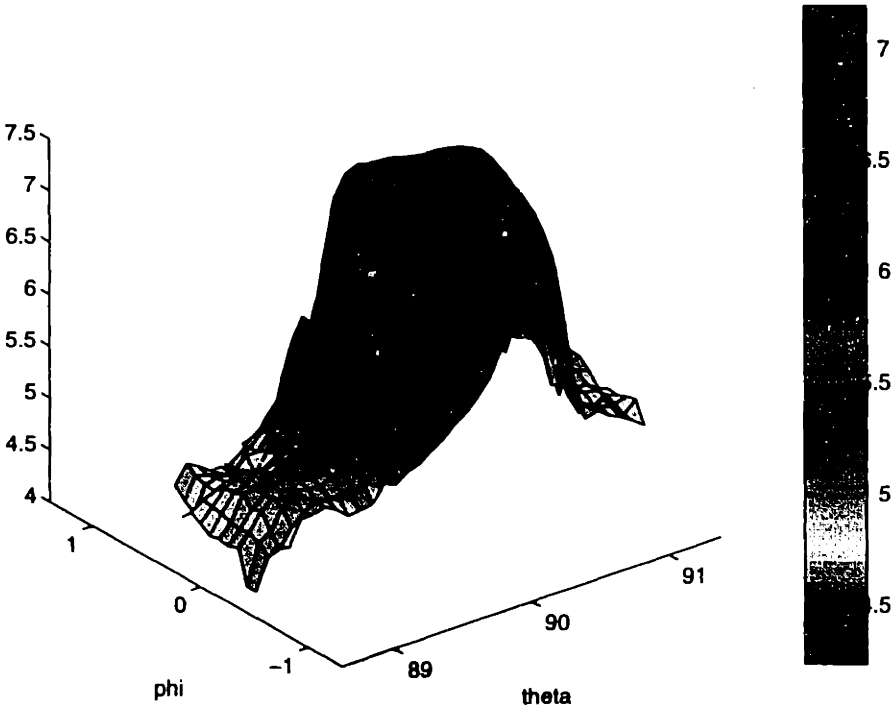


Figure 5-3: Field-of-View of the Pyroelectric Detector

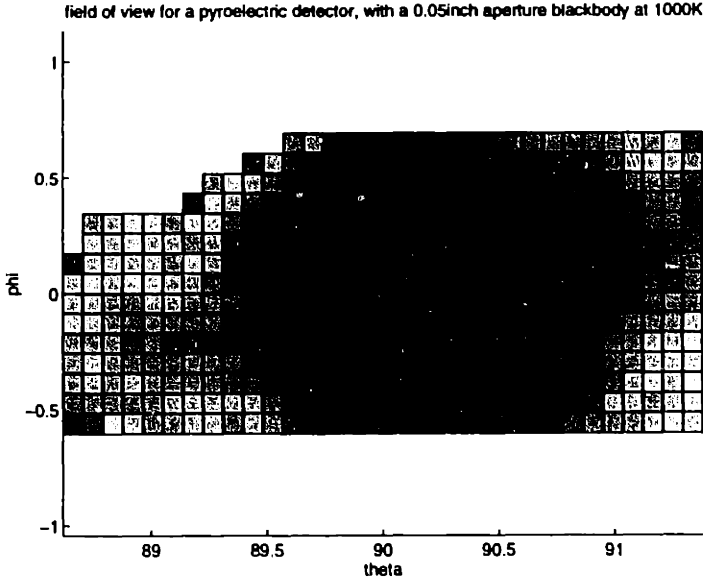


Figure 5-4: Field-of-View of the Pyroelectric Detector, Top View

5.5 Experimental results for the Lead Selenide Detector

5.5.1 Responsivity

Again, to evaluate the responsivity, the choppers were placed at the blackbody because when the choppers are located at the detector, the background is also chopped and this includes errors in the determination of the responsivity. Responsivity (and detectivity) were evaluated under the following conditions, with and without optics:

- Blackbody temperature : $500^{\circ}K$ for both cases; this is the temperature used by the supplier
- Chopper frequency : 100 Hz , 160 Hz and 1000 Hz
- Area of detector: 1 mm^2
- Cooler at 10 and $25\text{ k}\Omega$
- Noise level: 2 mV as a first approximation
- Spectral transmission of detector: boxcar between 3 and $5\text{ }\mu\text{m}$

A transmission factor of 80% is added when the optics are mounted. For the experiments, *without optics*, only the fan was used at 160 Hz . According to the frequency response (see next section) the responsivity (and detectivity) between 100 Hz and 160 Hz shows a very flat behavior. *With the optics* all three choppers were used. The experimental results obtained to derive the detectivity are shown in the following table. Note that the blackbody aperture used without the optics is bigger than when the focusing lens is used in order to get more signal on the detector.

	<i>Chopping frequency (Hz)</i>	<i>Thermistor value kΩ</i>	<i>Aperture(inch)</i>	<i>Signal (mV)</i>
<i>without optics</i>	160 Hz (FAN)	25	0.1	3.7 mV
			0.2	6.6 mV
			0.4	20.05 mV
			0.6	40.4 mV
<i>with optics</i>	100 Hz (FAN)	25	0.0125	7.8 mV
			0.025	31.35 mV
			0.050	124.4 mV
			0.1	503 mV
	100 Hz (slow chopper)	25	0.0125	7.540 mV
			0.025	30.85 mV
			0.050	126 mV
			0.1	522 mV
	100 Hz (fast chopper)	25	0.0125	9.24 mV
			0.025	33.85 mV
			0.05	129.8 mV
			0.1	497 mV
	1000 Hz (fast chopper)	25	0.0125	8.320 mV
			0.025	31.65 mV
			0.05	124.4 mV
			0.1	506 mV
	100 Hz (FAN)	10	0.0125	6.6 mV
			0.025	26.35 mV
			0.05	109.8 mV
			0.1	418 mV
	100 Hz (slow chopper)	10	0.0125	6.6 mV
			0.025	27.2 mV
			0.05	109.4 mV
			0.1	462 mV
	100 Hz (fast chopper)	10	0.0125	6.64 mV
			0.025	27.3 mV
			0.05	105.2 mV
			0.1	416 mV
	1000 Hz (fast chopper)	10	0.0125	6.560 mV
			0.025	26.55 mV
			0.05	102.8 mV
			0.1	395.5 mV

Table 5.2: Experimental Results for Responsivity Determination-Lead Selenide Detector

With a blackbody at 500° K, the irradiance between 3 and 5μm is⁴: 167.4W/m² or 0.01674W/cm².

Therefore, the incident power on the detector is:

$$Power = \frac{0.01674}{\pi} Aperture(cm)^2 \frac{\pi}{4} \frac{Area_{detector\ or\ lens(cm^2)}}{focal\ length\ of\ mirror\ (cm)}^2$$

which gives (without the optics)

$$Power = \frac{0.01674}{\pi} Aperture(cm)^2 \frac{\pi}{4} \frac{0.01^2}{105}$$

and with the optics (the diameter of the lens is 2 inches)

$$Power = \frac{0.01674}{\pi} Aperture(cm)^2 \frac{\pi}{4} \frac{2.54^2 \pi^2}{105}$$

The corresponding results obtained for the responsivity, the specific detectivity and the Noise Equivalent Power are shown in the following table and compared to the figures obtained by the supplier. Note that the supplier's calculations do not take into account the spectral transmission of the detector. Moreover, they give the optimal value of the responsivity and detectivity, calculated at high frequencies with a more accurate method (similar to the one presented at the end of this chapter) that does not include the electronics, which accounts for the difference between the experimental results and the specification values.

	<i>frequency (Hz)</i>	<i>therm. val. (kΩ)</i>	<i>Respons. (V/W)</i>	<i>D*</i>	<i>NEP (W)</i>
<i>without optics</i>	100	25	2.31e3		6.8e9
<i>with optics</i>	100	10	473	1.44e9	4.49e-6
	1000	10	455.5	1.35e9	4.79e-6
	100	25	567.8	1.77e9	3.65e-6
	1000	25	564.7	1.66e9	3.88e-6
<i>values from supplier</i>	1000	25	1.40e5	3.56e10	N/A

Table 5.3: Figures of Merit of the Lead Selenide Detector

⁴Using MAPLE function *int* .

5.5.2 Frequency Response

The frequency response of the PbSe detector was measured using a $500^{\circ}K$ blackbody, with aperture 0.1 inch. The detector was used in association with the focusing lens at a cooling level of $10k\Omega$. The results are shown in the following curves for the responsivity and the detectivity. Note that the values at 100 Hz and 1000 Hz have been calculated in the previous section and have been included.

Moreover, the difference between the two choppers has been corrected by rescaling the curve for the narrow chopper to the curve for the wide chopper that gives the highest numbers.

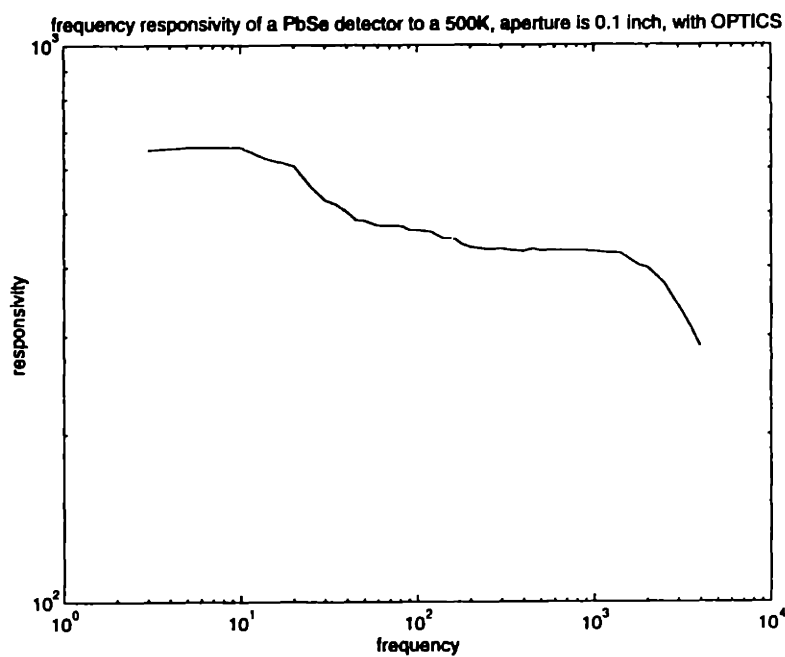


Figure 5-5: Responsivity of the Lead Selenide detector

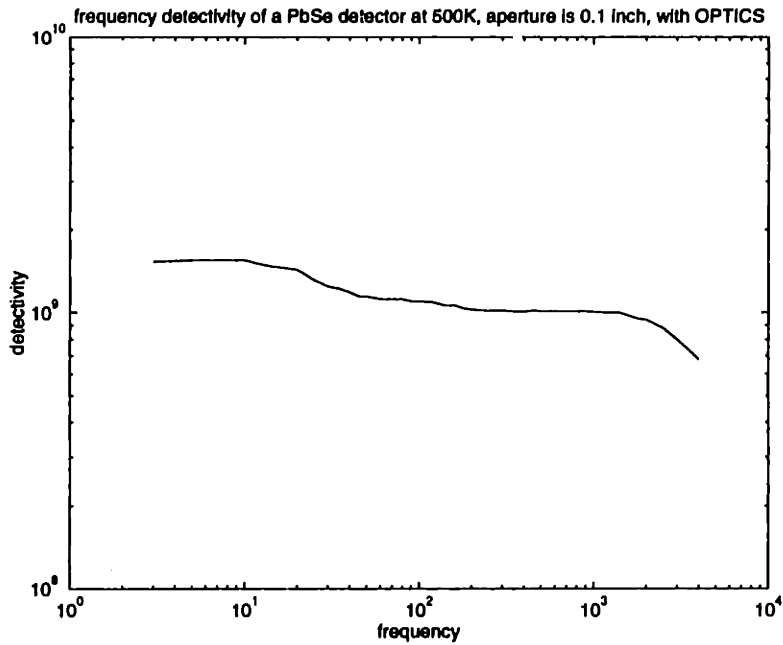


Figure 5-6: Detectivity of the Lead Selenide Detector

5.5.3 Field-of-View

The field-of-view was evaluated again with a 500°K blackbody using the optics. The angle for the field-of-view is here :

$$\frac{0.1}{10} = 0.01 \text{ rad} = 0.57 \text{ degree}$$

which is in agreement with the experimental results, that also show how the detector is oriented from the orientation of the square on the 2D plot.

field of view of a 1 mm² PbSe detector for a 773K detector, aperture is 0.2 inc

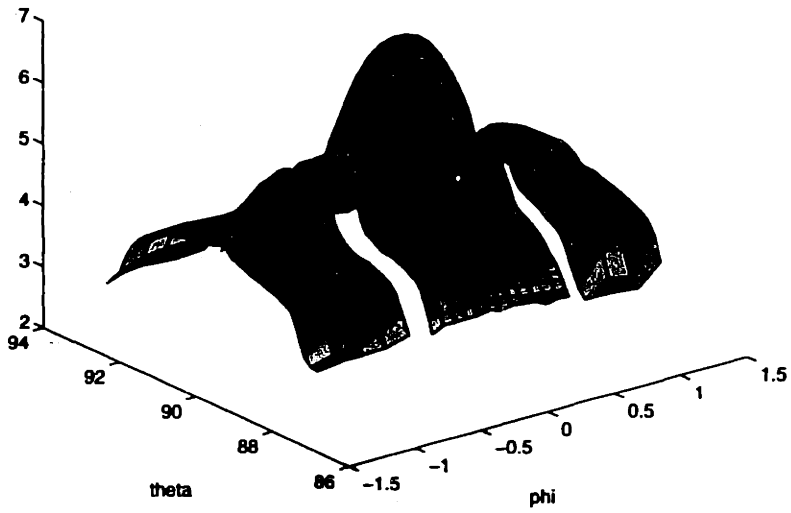


Figure 5-7: Field of View of the Lead Sellenide Detector

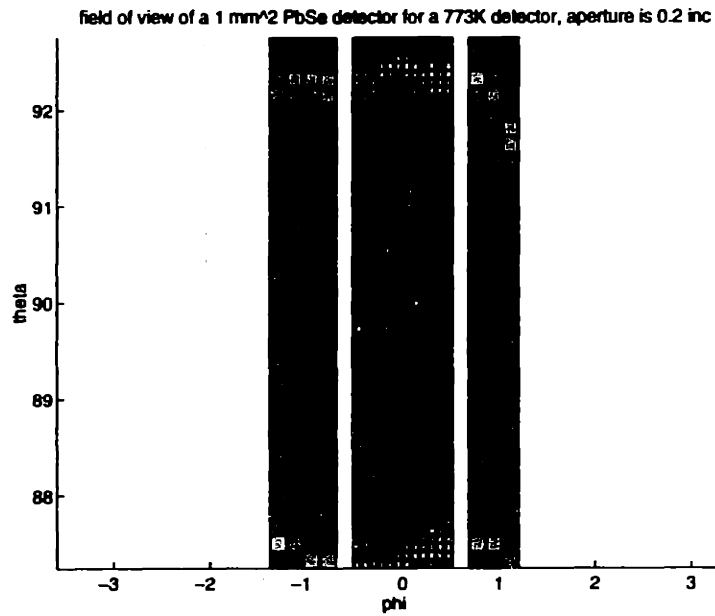


Figure 5-8: Field of View of the Lead Sellenide Detector, Top View

5.6 Experimental results for the MCT detector

For the Mercury Cadmium Telluride detector, only responsivity and field of view measurements could be achieved under conditions similar to those of the two other detectors.

5.6.1 Responsivity

The responsivity has been evaluated with optics under the following conditions:

- Blackbody temperature: $500^{\circ}K$
- Chopper frequency: 100 Hz using Fan chopper across detector
- Area of the detector: 2 mm^2
- Cooler resistance: $72.6\text{ k}\Omega$
- Gain of the amplifiers: 800
- Noise level: 15 mV

The signal(in Volts) measured by the oscilloscope as a function of the aperture of the blackbody is presented in the following table:

<i>Blackbody aperture (inch.)</i>	<i>Signal (V)</i>
0.6	2.230
0.4	1.555
0.2	0.517
0.1	0.1395
0.05 and below	noise

Table 5.4: Experimental Results for Responsivity Determination-MCT detector

Because the noise level was significantly higher than for the other detectors, the figures of merit for the MCT detector appear low:

- Responsivity: 104.8 V/W

- Detectivity: $4.17e7$
- Noise Equivalent Power: $1.059e - 4 W$

In the following section other values are derived from the noise spectrum analysis.

5.6.2 Field-of-View

The blackbody aperture used here was 0.2 inch with a chopper again at 100 Hz. The plots are the following.

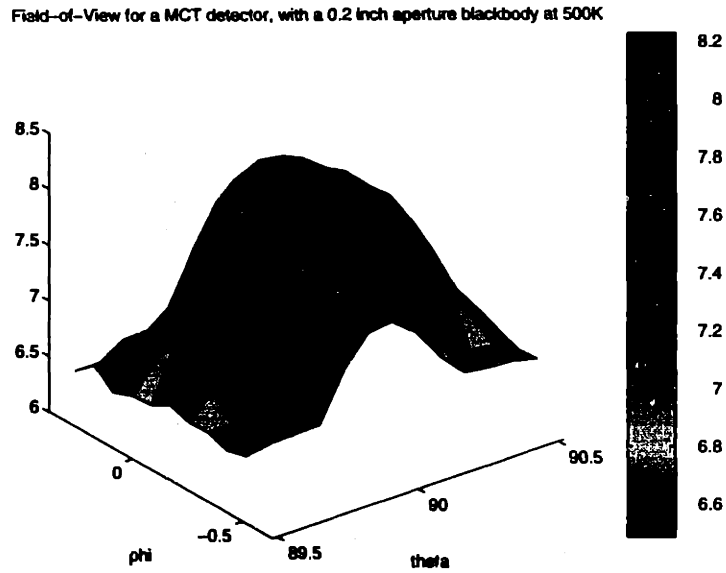


Figure 5-9: Field of View of the MCT Detector

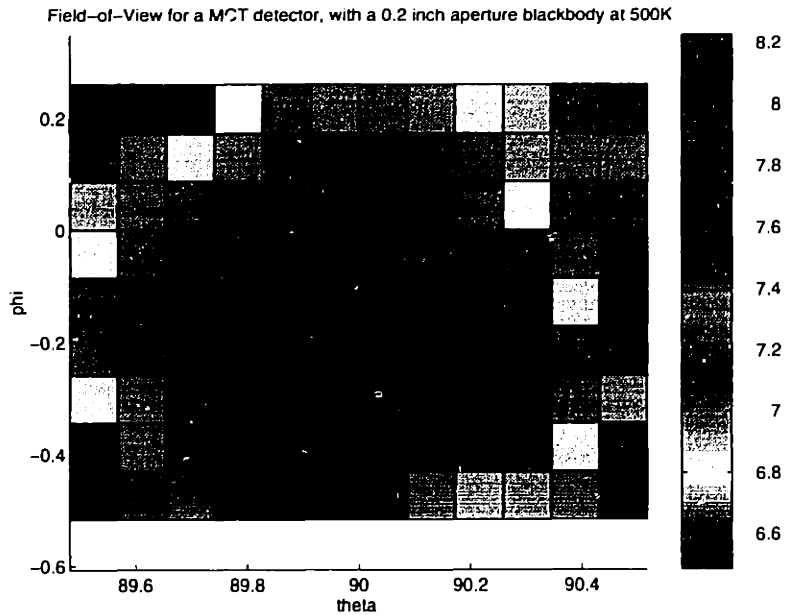


Figure 5-10: Field of View of the MCT Detector, Top View

5.7 Noise spectrum Analysis

In the above calculations, the rms value of the noise was assumed to be constant at a level of 2 mV . In fact, not only is the noise level lower, but it also decreases as the frequency increases. The noise spectrum and rms value have been evaluated based on a time series measurement for each detector. More accurate values for noise rms are:

- 0.969 mV for the Pyrodetector
- 0.477 mV for the Lead Selenide detector
- 0.250 mV for the Mercury Cadmium Telluride detector

The corresponding noise spectra derived from the time series data sampled at 50 kHz was smoothed with MATLAB function *psd* with a 1024-point Hanning window (50% overlapping has been used).

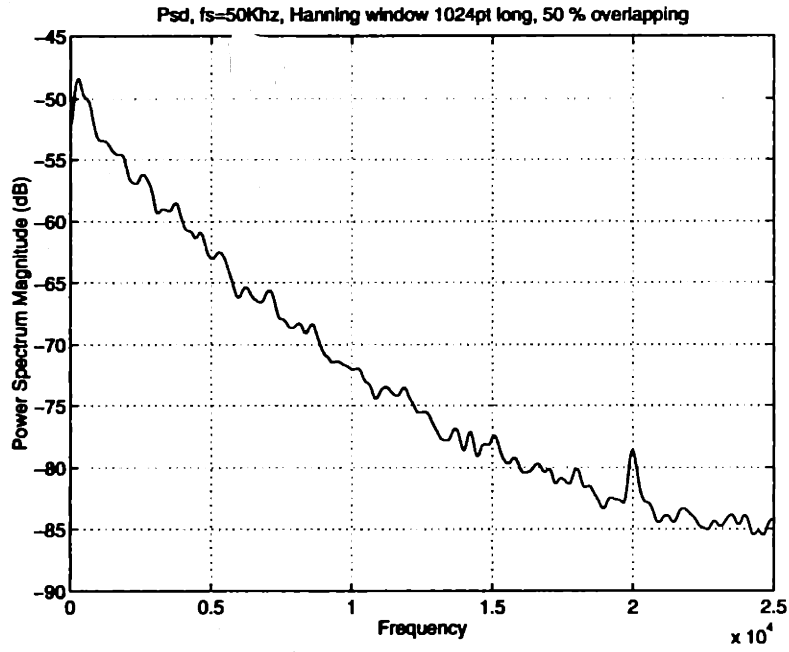


Figure 5-11: Noise Spectrum of the Pyroelectric Detector

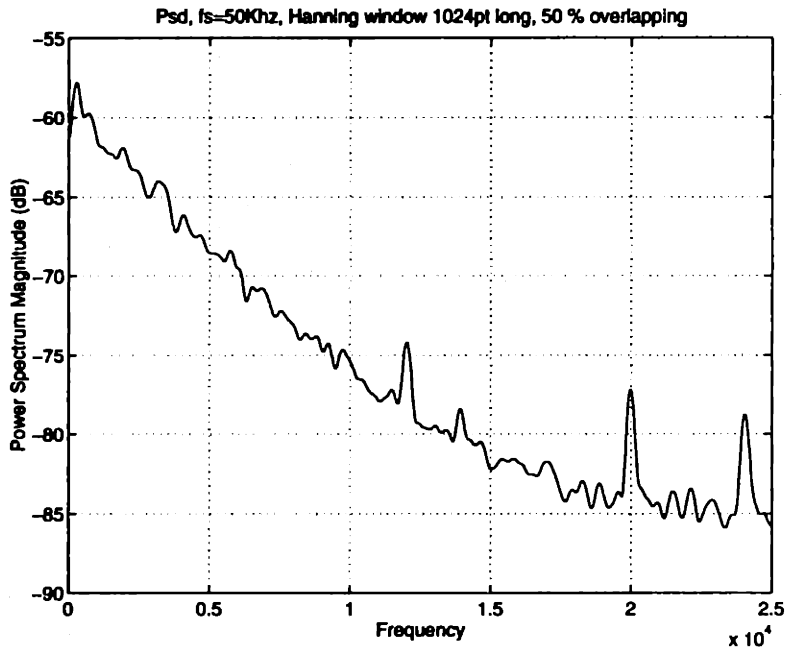


Figure 5-12: Noise Spectrum of the Lead Selenide Detector

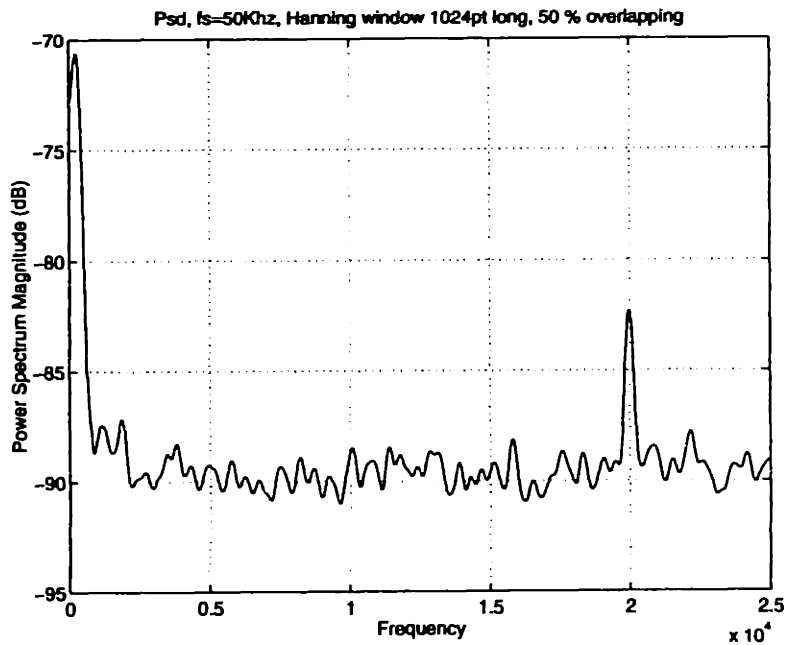


Figure 5-13: Noise Spectrum of the Mercury Cadmium Telluride Detector

Taking into account the real noise level and frequency dependence improves the detectivity figures, especially at high frequencies, as shown in the plot in the following page.

The new orders of magnitude for the figures of merit are, at low frequency:

- Pyrodetector

- Detectivity: $1.25e8$
- Noise Equivalent Power: $7.8e - 6 W$

- Lead Selenide detector

- Detectivity: $4e9$
- Noise Equivalent Power: $9.18e - 7 W$

- MCT detector

- Detectivity: $1.49e9$
- Noise Equivalent Power: $2.46e - 6 W$

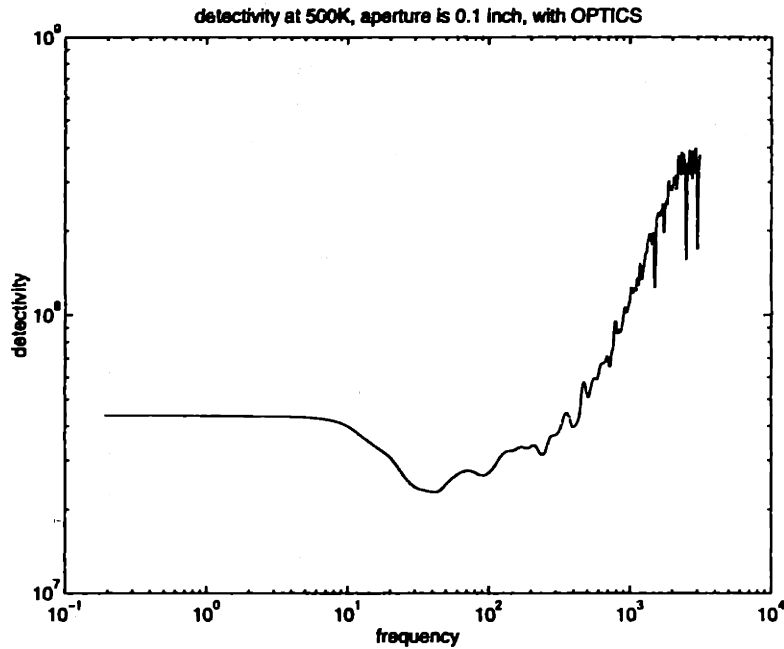


Figure 5-14: Detectivity of the Lead Selenide Detector Determined from Noise Spectrum Data

5.8 Effects of heating a window

An additional experiment was conducted to evaluate the consequences on the signal of inserting a hot window in the path of the beam coming from the blackbody. The experimental setup was similar to the one shown in figure 5-1, but for the inclusion of a 1-inch-diameter Zinc Selenide window between the two mirrors. A heat gun was directed towards the window producing different temperatures, measured by a thermocouple attached to the window. The signals with the heat gun off and the heat gun on were compared. Up to 90°C , the maximum temperature obtained, no modification of the signal was observed.

5.9 Field experiments

Once the calibration of the detectors was completed, the three detectors were mounted on a ground-based helicopter for a series of field experiments at night. The objective was both to verify the feasibility of the technology and to compare the performance of the three detectors. In this section, a brief description of the experiments is given. The problems revealed by the test are analyzed and the first results, processed at Visidyne, are discussed.

5.9.1 Experimental conditions

For the field experiments the three detectors considered were fixed together on the tail boom of an R22 (Robinson) helicopter. For the pyroelectric detector, sensitive to vibrations, vibrometers were added on the detector. Supercooled water droplets were sprayed on the detector using snowguns that could simulate different types of icing conditions. The detectors were connected through a coaxial cable to a data acquisition system, that collected information from the three detectors and the three vibrometers. To decrease the size of the files stocked in the computer, two special triggering systems were used that tracked the pass of the blade in the field of view of the detector. The first one was an optical trigger, consisting of a laser beam reflected by the blade to a photomultiplier tube. The second one was an inductive sensor, coupled to the RPM⁵ measurement system of the helicopter, that produced a track of the number of tours and therefore, of the blade pass.

The experimental setup sketch is shown in the following drawing.

⁵Rotations Per Minute.

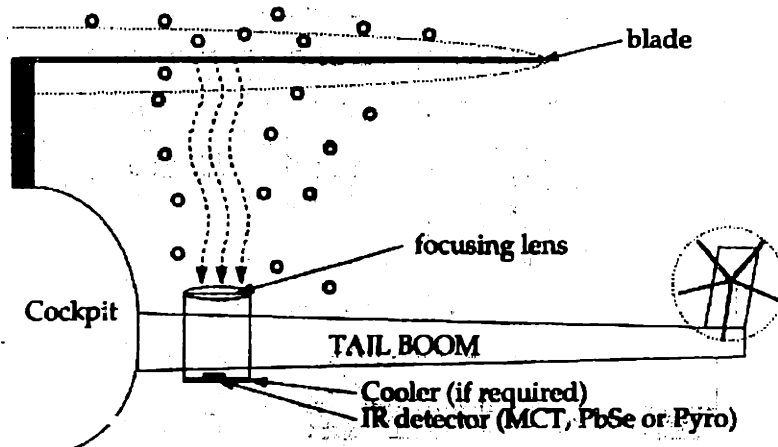


Figure 5-15: Field Test Setup

Different types of tests were run :

- Spray off/ Spray on test: for this experiment, the rotor was started for a few seconds before the snowguns were actually pointed at the detectors;
- Spray on/Spray off : in this case, the rotor and the snowguns were started at the same time;
- Spray off/Spray on, wet snow: for this test, the water content of simulated ice was increased;

Their objective was to evaluate the vibrations, the noise environment and, naturally, the ice detection capability.

5.8.2 Analysis of the experiments

Despite a good preparation , several problems appeared during the field experiments. Apart from trigger implementation difficulties, grounding problems resulted in noise addition to the signal. This was particularly critical for the pyroelectric detector. Moreover, the MCT detector did not work properly, so that the only results available are those from the pyroelectric detector, compromised by a high noise level, and those from the Lead Selenide detector. Though data

processing is not completed yet, the first results for the Lead Selenide detector seem to give a distinctive ice signature.

Since the detectors were looking up at the blades, they were directly facing the snow spray. Without any kind of sweeping, the signal from the blade was obstructed by the ice depositing on the lens⁶. Therefore it was necessary to blow nitrogen on the lens to prevent it from icing up. Not only did this require large quantities of nitrogen, but also it proved totally inefficient when the water content of the ice increased (wet snow). In that case, the lens was totally iced, once the test was completed.

In fact, the field experiments failed to validate the detectors, since they did not all work properly, but they underlined a series of weaknesses of the system that should be fixed for the design of the prototype. One of these is the icing of the optics. This issue is discussed in the following chapters.

5.8.3 Pictures

Some pictures of the field experiment setup and an example of ice on the blade are shown in the next pages.



Figure 5-16: View of the R22 Helicopter used for the Field Experiments

⁶Ice absorbs infrared radiation.



Figure 5-17: View of the Detectors Mounted on the Helicopter



Figure 5-18: Close-up View of the Detectors

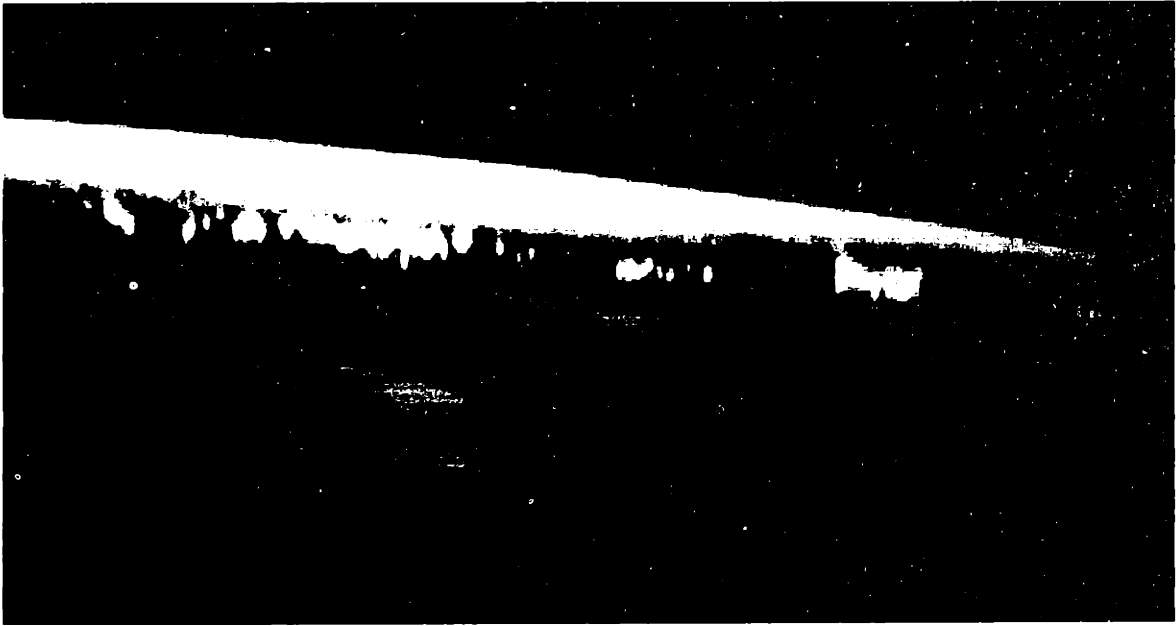


Figure 5-19: Example of Blade Icing (1)



Figure 5-20: Example of Blade Icing (2)

Chapter 6

Lens protection design considerations.

6.1 Background: relevance of a protecting subsystem, possible solutions.

As described in the previous sections, the ice detector considered to measure the ice build-up on the blade involves a lens (Germanium or Calcium Fluoride) that eventually ices up as well, as revealed by the field experiments. The Quality Function Deployment Matrix underlines that robustness to all-weather operation is an important requirement for the detector. Therefore a protective device should be implemented. For the field experiments, that were intended to check the detectors, a temporary solution was adopted. Nitrogen was blown on the detectors to prevent ice accretion on the lens. Of course this solution cannot be implemented because it requires large amounts of nitrogen to be efficient. The objective of this chapter is to evaluate alternate, more efficient solutions. Two main ideas are considered: a window protection mounted in front of the lens or a mirror that would deflect the incoming beam and prevent the lens from being directly exposed to icing. Historically, a third idea had been proposed by Visidyne, that consisted on a wiper mounted on the lens that would mechanically ¹ remove the ice, but this idea

¹As in car windshields.

was refused by NASA in an effort to minimize mechanical systems and will not be extensively discussed here. The relevance of these solutions depends on how well they perform, in terms of functionality, but also on how well they meet the requirements.

6.2 The heated window option

This protection proposes to heat either the lens of the detector system or a window mounted in front of the lens so that the optical component in contact with the environment (window or lens) does not ice up. One of the main concerns is the noise introduced by the heating system. This problem is common to the heated mirror option, described in the next section. Moreover, the choice of the window/lens material is particularly important to ensure a high transmission in the infrared range considered. In this section, a description of different materials leading to the choice of the one that seems optimal, is proposed. Methods to heat the window are also discussed at the end of the section.

6.2.1 Preliminary considerations

Using a heated window in an Infrared system could appear surprising because the power emitted by the source of heat might compromise the signal. It is revealing to observe how discrepant opinions are on this subject. Information from IR cameras suppliers, icing specialists and Army engineers emphasized the following contradictory points:

- Normally, in an infrared system, attention is paid to minimize the sources of heat in the field-of-view of the detector, therefore considering a heated device can appear as an uncertain option.
- A heated window should be no problem because detectors are sensitive to temperature variations (since they are AC coupled), so as far as the temperature of the coating remains constant, the detector should not see the information from the protection device. There are two objections though. First, it is not easy to maintain a constant temperature during the flight. Temperature variations may reach over 30 degrees C. Second, if the power emitted

from the window is higher than the expected signal from the blade then the background noise is going to blow out the signal.

- Heated protections have already been used for military tanks (M1 in particular) the major problem is to find a material transparent to IR radiation between 3 and 17 μm . A heated gold grid might be an alternative to the coating.

6.2.2 Noise considerations

The different sources of heat that should be considered to model the effects of a heated device are: the sky, the blade and the window. The sky can be assumed to be a blackbody at 240°K but the blade and the window are not perfect blackbodies and their spectral emissivity $\epsilon(\lambda)$ has to be accounted for in deriving the radiation they emit. When ice builds up, the temperature of the blade is around 273°K and the emissivity of the ice, considered as a gray body, is 0.97.

The temperature of the window is a factor of optimization and appears as a tradeoff between SNR, reliability and available power. Heating the window to 283°K seems an acceptable level to meet the previous requirements. The emissivity of the window depends on the material used. In the following derivations, this factor is a parameter.

As derived previously, the signal received by the detector without any perturbation is actually the difference between the power emitted by the blade and the power that falls into the field-of-view of the detector within the spectral bandwidth. This bandwidth varies from one detector to the other, which implies that the signal received by each detector is different. Taking into account the transmission factor of the optics, T_0 , and the F-number of the lens, the power received at the $1mm^2$ detector due to the real signal is:

$$\Delta W = \frac{T_0}{2 F^2} \left(\int_{\lambda_1}^{\lambda_2} \epsilon_{ice} \frac{2 c^2 h}{\lambda^5 \left(\exp \left(\frac{hc}{273 \lambda k} \right) - 1 \right)} d\lambda - \int_{\lambda_1}^{\lambda_2} \frac{2 c^2 h}{\lambda^5 \left(\exp \left(\frac{hc}{240 \lambda k} \right) - 1 \right)} d\lambda \right) \quad (6.1)$$

Using a transmission factor of 80 % and an F-number of 2, the expected signal from the blade is:

- 237 μ Watts for the pyroelectric detector (spectral window is 2.5 – 14 μ m)
- 0.76 μ Watts for the Lead Selenide detector (spectral window is 3 – 5 μ m)
- 61.7 μ Watts for the Mercure Cadmium Telluride detector (spectral window is 7.5 – 9.5 μ m)

If the detector is located at the focal point of the lens, the solid angle of the beam from the heated coating arriving on the detector is

$$\Omega = \frac{Area_{detector}}{f^2}$$

where f is the focal length ($f = 10cm$). The surface radiating can be considered as being the surface of the lens (here $A_{lens} = 2.03cm^2$). Hence the power emitted by the heated window at 283°K over the spectral bandwidth λ_1, λ_2 is:

$$W_{window} = \Omega \times A_{lens} \times \left(\int_{\lambda_1}^{\lambda_2} \epsilon_{coating}(\lambda) \frac{2 c^2 h}{\lambda^5 \left(\exp\left(\frac{hc}{283 \lambda k}\right) - 1 \right)} d\lambda \right) \quad (6.2)$$

Assuming a constant emissivity over the different spectra, the radiation from the window falling on the detector as a function of the emissivity is roughly:

spectrum	<i>PbSe</i> (3 – 5 μ m)	<i>Pyro</i> (2.5 – 14 μ m)	<i>HgCdTe</i> (7.5 – 9.5 μ m)
power (μ Watts)	0.197 $\epsilon_{coating}$	11.12 $\epsilon_{coating}$	2.72 $\epsilon_{coating}$
% of signal added	25.9 $\epsilon_{coating}$	4.69 $\epsilon_{coating}$	4.41 $\epsilon_{coating}$

Table 6.1: Percentage of DC Signal Added to Each Detector by a Heated Window

These figures reveal that the value of the emissivity is critical for the lead selenide detector. This calculation gives in fact the offset of the signal due to the heating device. Since the detectors are not sensitive to steady values of the temperature, the results obtained are an indicator of how important the signal is compared to the noise introduced by the the supporting system. Prediction of how the Noise Equivalent Temperature is modified by the presence of a source of heat in the field-of-view does not seem clear at this point.

6.2.3 Choice of materials

The choice of the material for the window is guided by the higher technical requirements obtained from the Quality Function Deployment Requirements matrix. Other considerations are also important for the choice of infrared window materials as described by [KOK] and [12]. Therefore a more complete set of requirements for the choice of the window material is:

- high transparency in IR range
- high refractive index, independent of temperature
- zero dispersion
- zero coefficient of thermal expansion
- high surface hardness
- mechanical strength
- chemical stability

In practice, no material meets all the requirements at the same time and it is considered satisfactory to have two of the above properties satisfied at once. It is therefore important to understand what effects the different properties of the materials and how critical they are for the performance of the window/detector before any trade-off is decided.

Transmittance Window

One of the limits to the transmittance window of a material is determined by how the electrons in the valence band react with the incoming electromagnetic radiation. For metallic conductive type solids, the electrons are easily excited by the radiation and these materials are opaque over a wide frequency (wavelength) range. Insulators or semi-conductors exhibit an energy gap between the valence band and the conduction band. In this case, the electrons from the valence band will jump to the conduction band only if the energy of the radiation exceeds the energy gap. Therefore, these materials are transparent up to a frequency cut-off level or beyond a

wavelength cut-off, λ_c that is determined by:

$$\lambda_c = \frac{h c}{E_{gap}} \quad (6.3)$$

where h is Planck's constant and c is the speed of light. There is another practical limitation for the transmittance window that is set by the thermal excitation of the vibrational modes of the structural lattice in the mid to far infrared. Depending on spectral transmission, materials can be divided into three groups. The first group is sensitive up to $3 \mu m$ (near infrared), the second up to $5 \mu m$ (mid infrared) and the third, is transparent up to $14 \mu m$ and beyond (far infrared). The different kinds of possible materials for infrared windows and their characteristics are shown in the following table.

<i>Material</i>	<i>Bandgap</i>	<i>refractive index</i>	<i>absorption coefficient</i>	<i>coeff. of thermal expansion</i>	<i>mechanical strength</i>	<i>chemical stability</i>
halides	high bandgaps ⇒ transparency to UV, visible, IR	low-medium	low	low	poor	poor
oxides	medium bandgaps ~ 3-6 eV	medium : 1.5-2	low	good	good	good
chalcogenides (S, Se, Te)	low bandgap <3 eV	medium-high :2-3	low	moderate	moderate	
semiconductors	low bandgap ~ 0.7-2.22 eV	medium-high	high	moderate	moderate	good
others (nitrides, borides sillicides, carbides)				good	good	very high melting point

Figure 6-1: Comparison of the properties of different materials for infrared windows

The relative properties of the different categories of materials and their transmittance window are displayed in the following figures adapted from [12].

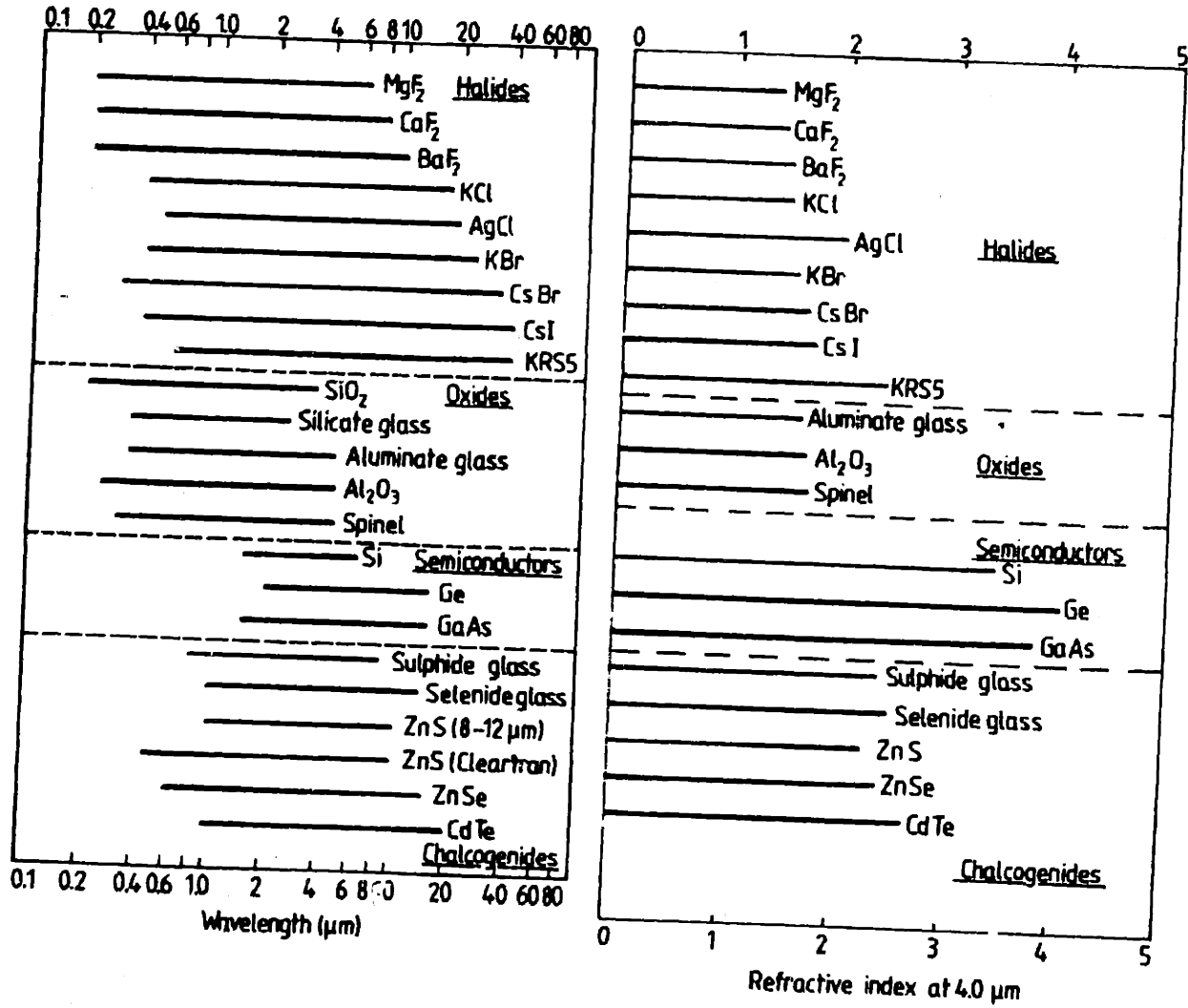


Figure 6-2: Spectral Window (left) and Refractive Index (right) for Different IR Materials

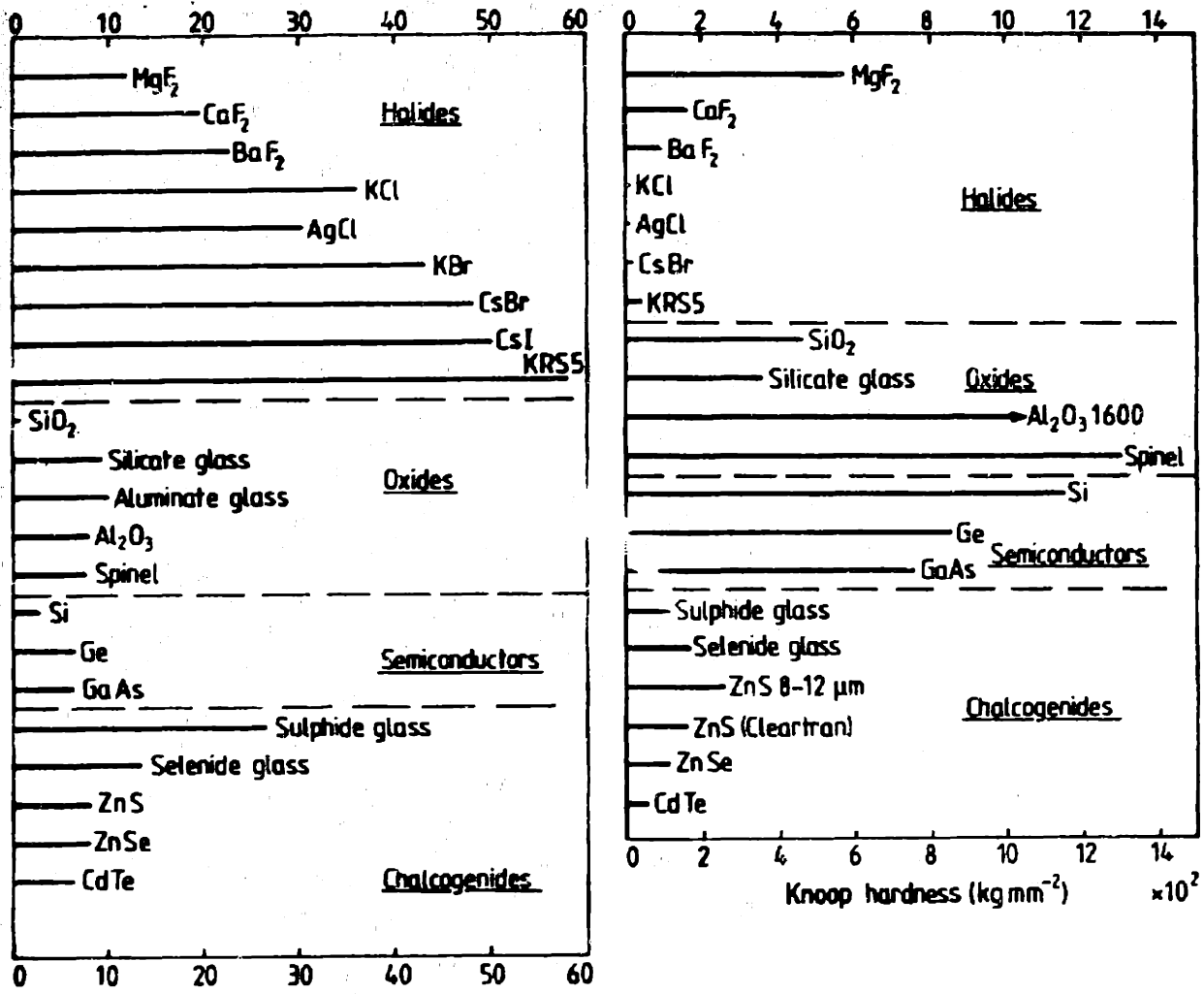


Figure 6-3: Coefficient of Thermal Expansion (left) and Surface Hardness (right) for Different IR Materials

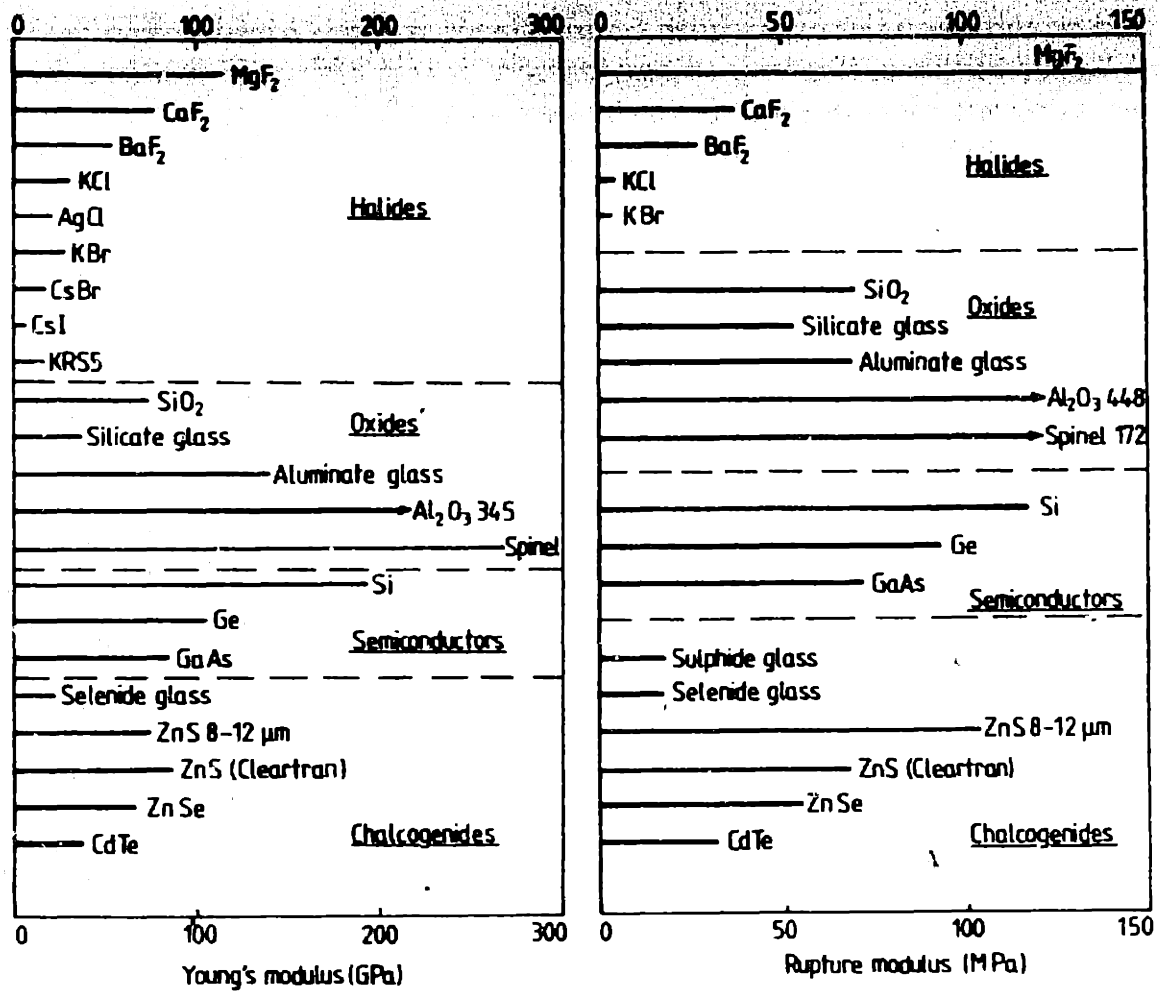


Figure 6-4: Young's Modulus and Rupture Modulus for Different IR Materials

This comparison reveals that oxides are not good candidates for mid-far infrared windows. Halides have wide spectral windows but their thermal expansion coefficient is relatively high, except for Calcium Fluoride and Magnesium Fluoride, for the mid-infrared region. The more suitable materials for the far-infrared spectrum are semiconductors and chalcogenides glasses. The properties of these materials should be studied in further detail before choosing the best candidate.

Materials for a mid-far infrared window

Any choice of the material for the window is strongly correlated to the selection of the detector. Mercure Cadmium Telluride and the Pyroelectric detectors have large spectral windows that extend to the far infrared whereas the Lead Selenide detector is sensitive to mid-infrared radiation only. Semiconductors and chalcogenides are transparent to the mid and far infrared radiation but their refractive index is significantly high and the use of an halide with a small thermal expansion coefficient might appear more convenient if the Lead Selenide detector is selected. The different possible materials, with multispectral capability are examined in the following section. However, only multispectral materials are considered in the following study.

Mid-Far-infrared materials

- **Germanium**

This material has major optical assets : high transmittance up to $15 \mu m$ and low dispersion, which allows to avoid chromatic aberration corrections. Moreover the mechanical properties in terms of hardness and strength are good and the thermal conductivity is high ($167 \times 10^{-3} cal cm^{-1} s^{-1} K^{-1}$). However, the use of this material for the detector window might not be accurate since:

- The thermal expansion coefficient is high: around $6.1 \times 10^{-6} K^{-1}$
- Transmittance degrades with the temperature and beyond $70^{\circ}C$ the material becomes opaque because of free-carrier absorption. Therefore, if heating is significant, Germanium should not be chosen. It should be noted that heat can come either

from the warming system used for the particular application considered here, or from aerodynamic heating that should not be significant at low speeds.

- According to [12], long exposure to rain degrades the transmitting properties of the material and might result in visible surface damage.
- **Gallium Arsenide** This material offers high transmittance (comparable to Germanium) between 2 and 12 μm . Because the bandgap is higher than that of Germanium, Gallium Arsenide does not suffer from heating below 200° C. Besides a high thermal conductivity ($84 \times 10^{-3} cal cm^{-1} s^{-1} K^{-1}$), this material is rather hard. In-flight damage comparison reveals that for a given number of flight hours, degradation of transmittance is lower for Gallium Arsenide than for Germanium (as reported by [12]). If T_0 and T are the pre-flight and post-flight transmittance, the damage results for coated specimen are shown in the following table, in which transmittance was measured at 10 μm as a function of the total flight time in varying external conditions ranging from clean dry air to rime-ice to sandstorms ².

<i>Total Flight Time (h)</i>	<i>T/T₀ at 10 μm</i>		
	<i>GaAs</i>	<i>Ge</i>	<i>sample</i>
200	0.955	0.944	uncoated
343	0.918	0.800	coated
618	0.859	0.733	coated
822	0.937	0.555	coated

Table 6.2: Comparison of the transmittance for GaAs and Germanium windows as a function of flight time

This table shows that Gallium Arsenide is better suited for flight applications than Germanium as long as the spectral window of the detector does not exceed 12 μm , which excludes the pyroelectric detector. Yet, this material has a series of major drawbacks, that include:

- high thermal expansion coefficient: $5.7 \times 10^{-6} K^{-1}$,

²see [12] p.79

- sensitivity to rain impact: specimens of GaAs show erosion and fracture when exposed to simulated rain drops to a larger extent,
- high cost.

- **Chalcogenide Glasses** Chalcogenide glass is a generic name for materials containing one or more of the chalcogenide elements Sulphide, Selenide or Teryllium in association with Germanium, Silicon, Arsenic or Sb,... (and some others). Research on these materials is recent, and little systematic work has been done on some of their properties such as thermal conductivity, hardness, elastic moduli and mechanical properties. They appear as a good passive optical component for the range 8 – 12 μm .

Among them sulphide glasses appear to offer good transmission up to 11.5 μm which does not cover the whole far infrared spectrum. Selenide glasses have a larger spectral window, but their optical properties, in terms of refractive index can be improved by mixing Selenide and Telluride to yield Selenide-Telluride glasses. Telluride glasses, transmit further in the infrared but their production proves difficult.

The physical, thermal and mechanical properties strongly depend on the composition of the glass. However, it appears that these glasses are not physically and thermally robust, which precludes their use as window components exposed to harsh environments.

- **II-VI Compounds** These compounds include Cadmium Sulphide, Zinc Sulphide, Zinc Sellenide and Cadmium Telluride. Their properties depend on the production process: hot press polycrystalline solids (Irtan materials developed by Eastman Kodak) or Chemical Vapor Deposition (CVD). Zinc Sulphide and Zinc Sellenide offer the major advantage of having a multispectral capacity (specially when grown by vapor process) in the mid and far infrared. Their transmittance can reach 70 % from around 0.4 – 0.5 μm to 20 μm (with a special treatment) as shown in the following curves adapted from [12].

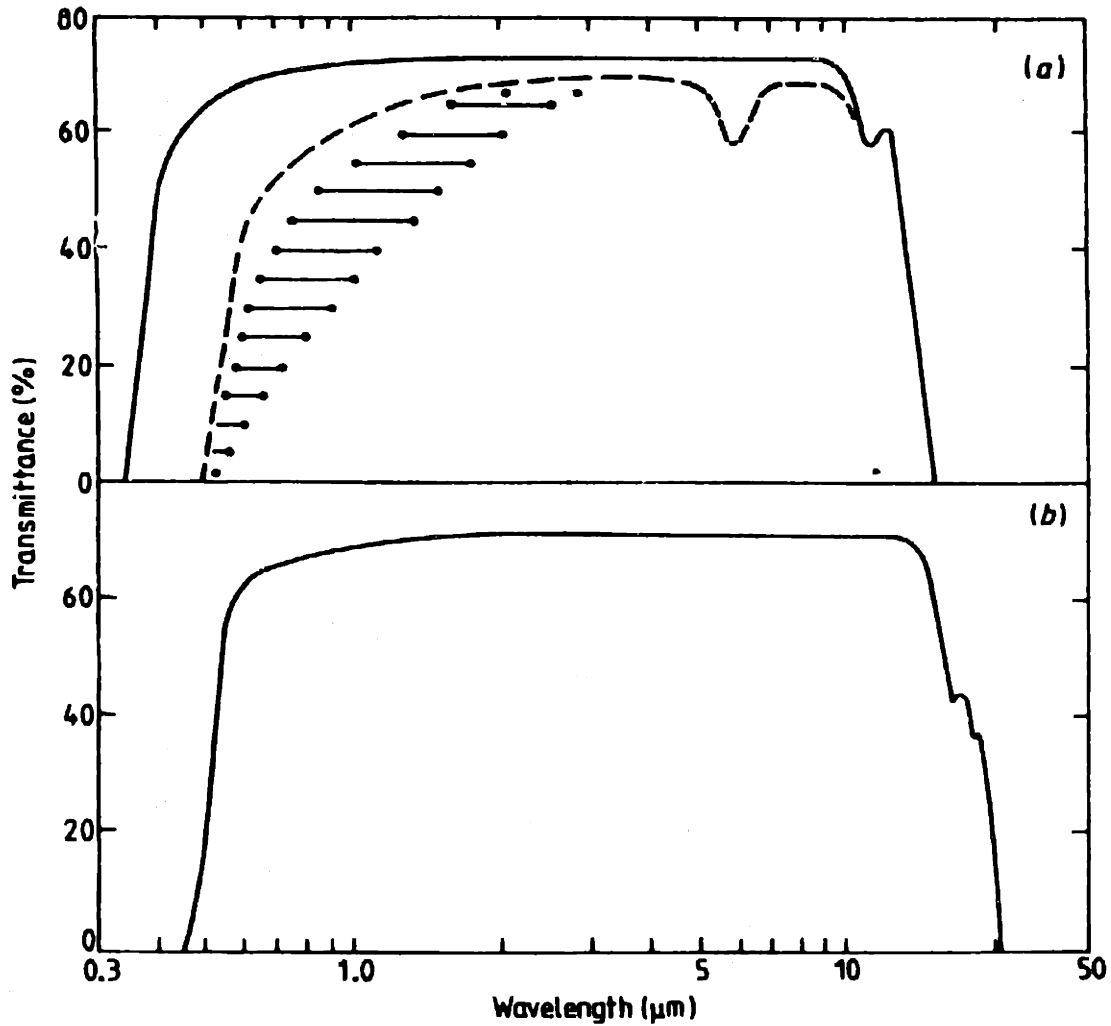


Figure 6-5: Transmittance of CVD ZnS 6 mm Thick, Multispectral Curve (top); Transmittance of CVD ZnSe 10 mm Thick (bottom)

Zinc Sulphide has good optical, thermal and mechanical properties at ambient temperature, but degradation of optical properties is observed at high temperatures (a few hundred degrees centigrade), though no detailed high temperature study has been done. Also, transmittance is reduced by rain erosion at high impact angles or impact velocities. In fact, the impact velocities for which optical degradation is significant are much higher than the average cruise speed of a helicopter. Infrared properties of Zinc Selenide glasses are better than those of Zinc Sulphide, specially beyond $10\ \mu\text{m}$ but the strength and hardness of this material is about half those of ZnS. Moreover, it critically suffers from rain erosion damage. A compound associating Zinc Sulphide and Zinc Selenide with improved optical

and rain resistance properties has been imagined but technical production problems have to be solved.

- **Diamond** Diamond appears as the best infrared material for its optical and mechanical properties. It has been used for window applications on space vehicles essentially, for which thermal and mechanical environments are rugged. Moreover it has multispectral capability when sufficiently pure, with a transmission range from the ultra-violet to the infrared. The main drawbacks of this material are related to its scarcity and high cost.

This analysis shows that for an aerodynamic window application in possible adverse environments requiring heating, Germanium and Chalcogenide glasses are not well suited. Diamond has deterrent costs. Gallium Arsenide appears as a good candidate, but Zinc Sulphide might be preferred for its multispectral capability, cost and availability³. More suitable materials might emerge from the current investigation on rare earth ternary sulphides, that would offer better overall physical, multispectral properties, but with current technology, Zinc Sulphide might be the optimal material for a heated window protection, regardless of which detector is used.

6.2.4 Choosing the heating device

As stated in the introduction of this chapter, heating the optics is not the only possibility to prevent the system from icing up but it appears as the more intuitive proposition, since the mechanical solution proposed by Visidyne was dismissed by NASA, the main contractor⁴. Any solution based on blowing cold air will not be considered either because the field experiment revealed that it required too large amounts of air and was not even efficient for some extreme conditions.

Different solutions remain for the choice of the heating device, that will be examined here: a heated coating, a hot air blowing system and a built-in electrical heater.

The heated coating system is simply a thin continuous conducting film, chosen for optimum heating, covering the lens (i.e. no extra window is required). In fact, this solution is not adapted

³Zinc Sulphide/Selenide materials are high quality off-the shelf optical materials

⁴See rieder1.

to multispectral detection: it is designed for single wavelength radiation transmission. Moreover it considerably attenuates the signal. Therefore, it should not be considered any further.

In different applications, where deicing is required, hot air is blown on the surface to be defrosted. In particular, engine inlets on helicopters benefit from the hot air taken from the engine compressor and sent via ducts to the ice-sensitive surface. This solution is often preferred to electrical devices because it saves electrical power, that appears more penalizing. A similar system could be implemented to blow air on a protective window. It will be referred to as the "bleed air concept" in the following sections.

Actually, the problem of heating infrared optical systems has been studied for many years for military applications. To protect the infrared camera of the M-1 A-1 tank, supposed to work in multispectral mode, a solution was adopted based on a gold grid heater built in the window. This kind of system is close to the one used in some windshields (cars or airplanes), but the gold mesh technology has been optimized for infrared windows applications. Information on this technology is very rare as it has been used in military applications exclusively. There is experience on gold mesh systems implemented on quartz materials at Litton Electro-Optical Systems⁵. Evaporated Coating claimed experience on Indian Zenoxyde and Mark Michell at General Dynamics Land Systems⁶, who was in charge of the design, stated that Zinc Selenide and Sinc Sulphide windows were well suited to the use of a gold grid. There are two kinds of grids: the heater and the gold grid EMI protection. The first one, with a current applied on it, has a defrosting capability; the second one, thinner, is used to diffuse to the ground, acting as an EMI shield insulator. For military applications, both grids would be required, in which case they would be implemented like a sandwich: one layer heater grid covered by an attenuator in RF band (shield insulator) covered by another heater grid. For civilian applications, in which stealth is not a major issue, the EMI insulator can be omitted. This method should keep from freezing down to $-60^{\circ}F$ ($-51.1^{\circ}C$), with a temperatures applied as hot as $120^{\circ}F$ ($49^{\circ}C$). Limitations in size for the utilization of this method include a practical limit in the grid size set by the limits of lithography. This means that the spacing in the grid should be at least $17\ \mu m$. Moreover, special care should be taken so that the grid does not become an antenna, which restricts the

⁵Note that these materials have not been considered for our window.

⁶See List of Contacts in appendix.

spacing of the grid to lengths higher than the wavelength. For infrared applications, this is not a limitation given the technology limit imposed by lithography. Besides, the grid resistane should be kept as constant as possible, in order to avoid temperature fluctuations on the window and possible extra-noise in the signal.

6.3 The mirror option

Protecting the detector system with a heated window assumes that the detector is looking up at the blades. In fact, if some device reflected the beam from the blade to the detector, there would be no need to face up the blade and be exposed to ice. This device could be a mirror with high reflectivity in the infrared (as derived from the technical requirements priorities). In that case, the mirror would possibly be subjected to icing, so again a heating device is needed. A sketch of the idea is shown in the following figure.

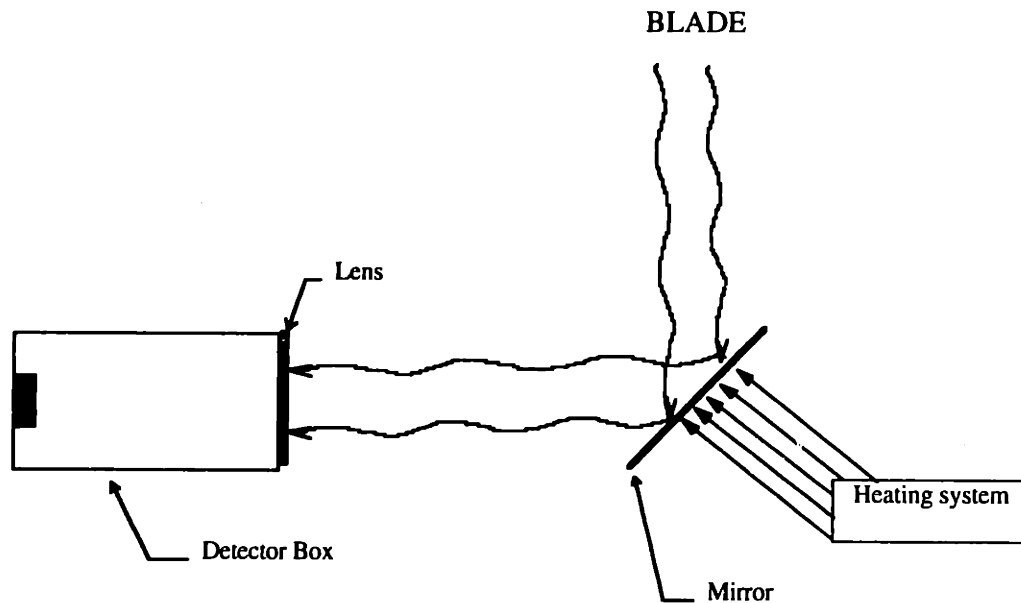


Figure 6-6: Sketch Of The Mirror System Implementation

Again, the heat from the mirror will introduce noise to the signal, that seems comparable, in terms of blackbody radiation to the noise added by the window. However, there is no simple way to predict the noise level by calculations.

With the heated mirror option, the choice of materials is not as complicated as for the

window. To ensure high reflectivity in the infrared spectrum considered, the mirror should be coated with gold ⁷, that has a reflectivity of about 95 %. In addition, special attention should be paid to two points. First, in order to improve the strength of the mirror surface, gold protection, besides gold coating is required. This is a reinforcement that prevents surface scratches. It seems all the more critical as the mirror will be submitted to a rugged environment. Moreover, not all the mirrors can be heated, without any possible consequence. A special treatment is required that also allows setting the limits of heating.

For the mirror, electrical heat can be supplied by glueing a heating blanket to the back of it. This type of blanket can come in different sizes or shapes easily adaptable to the mirror⁸. The power available from the heater depends on the blanket resistance and on the way it is attached to the mirror, which determines how well heat conduction is achieved. A few Watts can be easily obtained to heat a 12-square-inch mirror. The correspondance with heating temperature is not straightforward and should be determined from experiments.

⁷Aluminum mirrors are not well suited to infrared applications.

⁸Minco, Inc. is a splier for this kind of heaters.

Chapter 7

Design integration and preferred concept

Three implementations of the solutions for the protection of the lens discussed in the previous chapter, have been considered. Two of them are related to a window-type protection and the third one is based on the heated-mirror system. In all cases, the detector coupled to an F-1 (1 inch diameter, 1 inch focal length) lens is as independent of the protective device as possible. This is straightforward for the mirror option, but in the case of the lens, an extra window is not explicitly required and heating the lens directly was one of the first choices. In fact, this might not be relevant, because the effects of the heat on the lens (expansion for example) can degrade the accuracy of the optical setup.

Moreover, in deriving the possible implementations, special emphasis was put on the design for manufacturing, assembly and especially serviceability. This might have been at the expense of some extra weight, that seemed negligible given the size of the object considered. In this chapter, these implementations are described. A possible integration in the helicopter is then proposed, for the particular case of Eurocopter SuperPuma. Costs of implementation are also estimated at this point. Finally, a concept comparison is proposed on the basis of the discussion covered in these last two chapters.

7.1 The gold grid protection

In this case, the design is based on a double box system. The internal box contains the detector and a screw system to adjust the focusing of the lens that is attached to the inner part of the external box, through a screwable ring. These two boxes are combined through a set of screws and a cover fixed at the bottom. The window is mounted on the top of the external box and can be accessed directly just by removing a cover. To ensure that water stemming from ice melting will be removed, the depth of the window within the box is as small as possible so that it can be exposed to the relative wind. The robustness of the material is then important.

The free space between the two boxes allows to put the wires to power the gold grid as well as the thermocouple wires.

The shape of the upper part of the box is designed to mount the detector on the helicopter skin with screws (the trace of the screw is symbolized by the dash-dotted line).

A view of this concept is shown on the following sketch. Note that dimensions have not been determined with accuracy.

To prevent water (rain, melted snow/ice) from entering the detector box, an isolating seal should be mounted around the window.

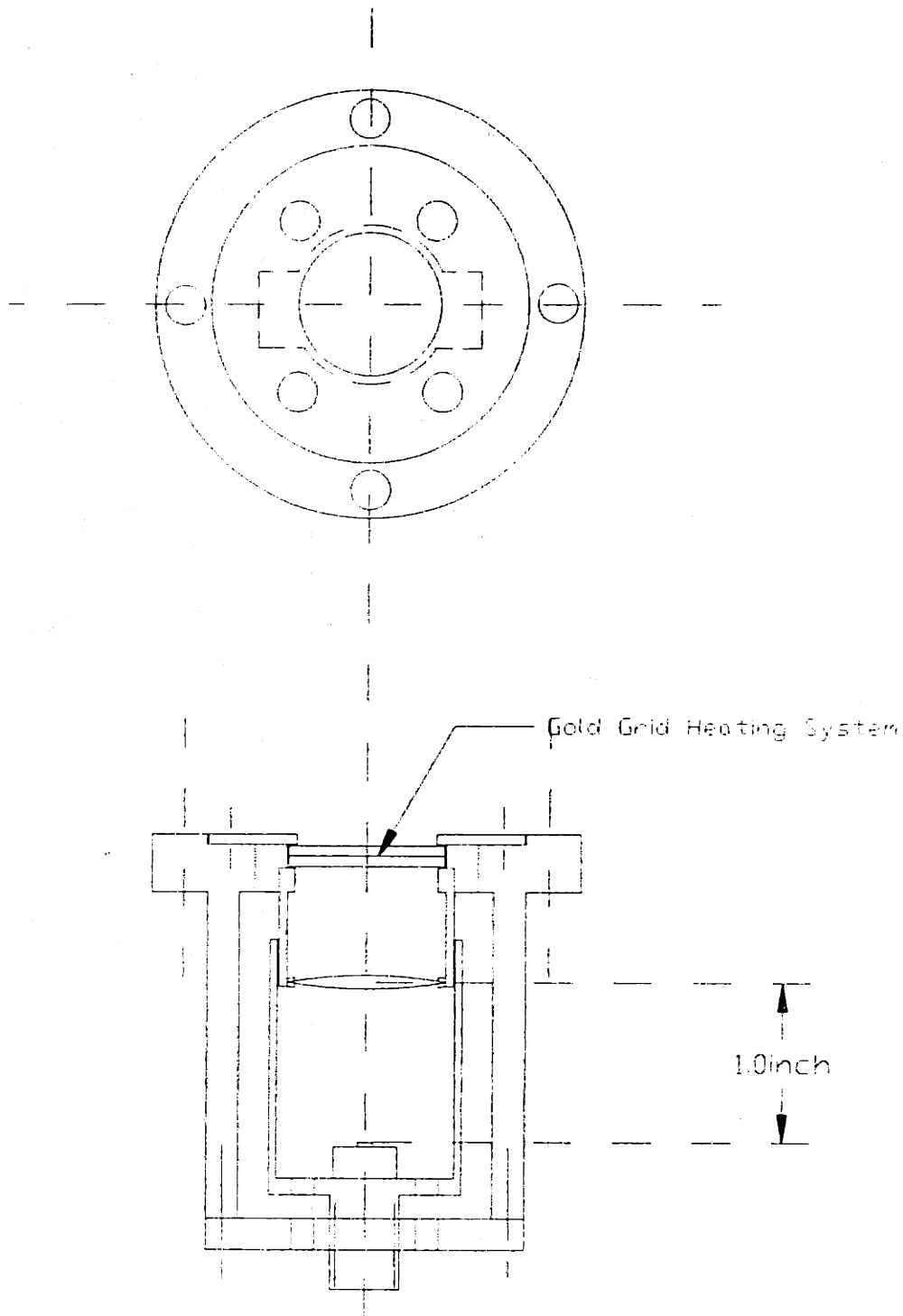


Figure 7-1: Gold grid heated window concept

7.2 The bleed air concept

For this solution, the design is very close to the previous one. The difference lies on the top of the box, which is stretched to allow for space to place the ducts coming from the engine. Note that the ducts are not included within the box of the detector, which is likely to facilitate maintenance. The result is represented in the following figure.

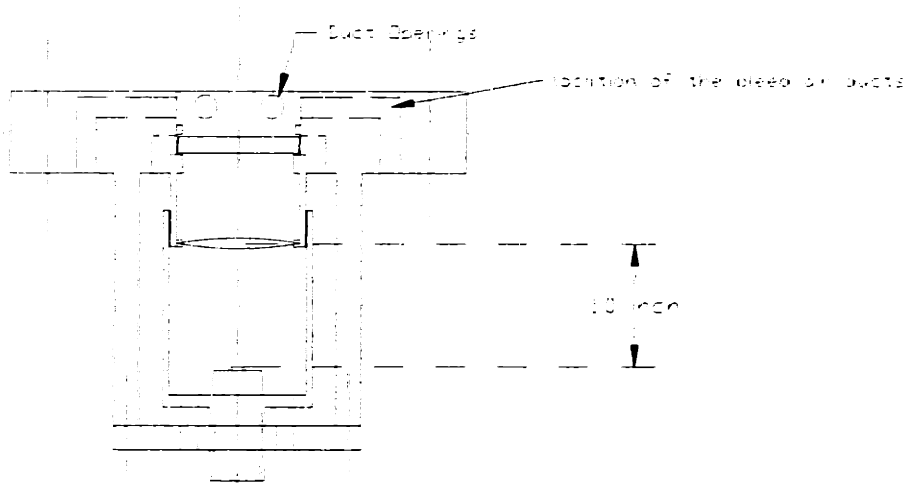


Figure 7-2: Bleed Air Concept

Tubes connecting the detector to the engine are not represented here, but a special setup is required to link the detector's duct and the compressor, that would involve some plumbing and possibly complex mounting. This solution seems all the more attractive since the detector is mounted close to the helicopter engines.

7.3 The heated mirror concept

To facilitate the handling of the detector system, it seems useful to include both the detector and the mirror in a box that can be opened for operations and closed on the ground to prevent the entrance of dirt. Handling of the mirror, specially, requires much care. For maintenance purposes, it is preferable that the mirror and the detector can be removed from the box independently. Therefore, special openings on both sides of the box have been made. The actual

design of this concept is related to the way the integration on the helicopter will be achieved. Since the detector and the mirror are mounted side by side, a larger area in the helicopter is needed to place the system. A convenient way to put the detector-mirror system would be to have it sitting on the skin of the helicopter as in the previous cases. Other types of mounting, that would reduce the size of the skin area used by the detector, such as putting it underneath the skin surface, would also require hatches. Moreover, access to the detector for maintenance would be more difficult.

A sketch of a proposed design is shown in the following figure.

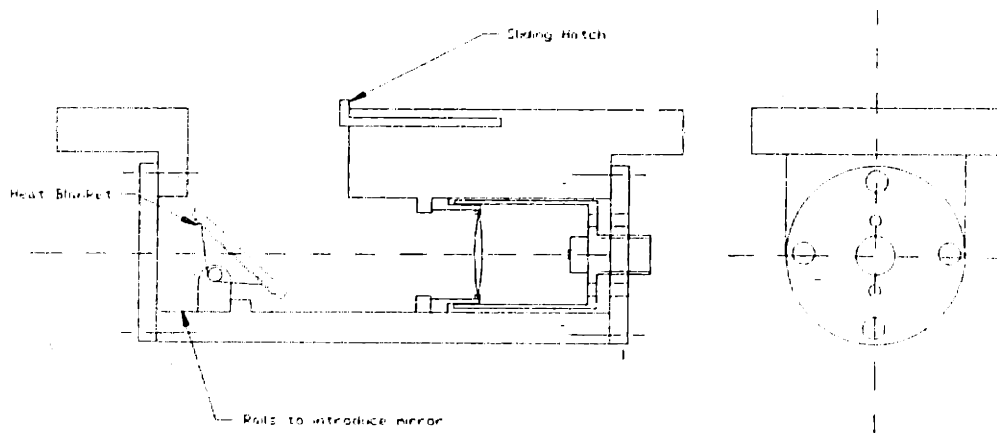


Figure 7-3: Mirror Concept

7.4 Possible integration on the helicopter

A first attempt to choose a universal location for the detector that would be valid for any helicopter proved inefficient because helicopter features are very different from one type of aircraft to another. For the field experiments, the detectors were mounted on the tail boom of the R22 helicopter. Whether this is a possible definitive location will be examined and other possible locations will be suggested in this section, considering the example of Eurocopter Super Puma.

Several questions arise when trying to determine the way the detector is going to be mounted on the helicopter and the optimal location for it. Among them:

- Should the detector be sticking out of the helicopter or should it be built inside ?
- If the detector is mounted "outside", is the drag penalty significant?
- If the detector is mounted inside, is the subsequent hole on the helicopter skin compatible with the mechanical structure ?
- If a hole is required on the helicopter, should the structure at that point be reinforced ?

Given the size of the detector, the drag increase induced by the detector protuberance, would not be significant. In fact, helicopter design is not aerodynamically optimized. For some of them, diverse large antennas degrade the aerodynamic performance. Therefore, even if the detector were to be mounted outside the helicopter, the drag increase would not be important compared to other devices. However, there is no advantage to fixing the detector outside the helicopter if it can be integrated inside. The design of the detector box is oriented towards this option. In this case, the problems are structural.

Drilling a hole in the skin of the helicopter sets a double structural problem. First, at the designated mounting point, the skin of the helicopter should not be a structural support, that takes the loads. At this location, an internal beam or a solid structure is required. Besides, some parts of the helicopter would require structure reinforcement if a hole were bored in them, so it would be preferable to have the detector on one of the parts of the helicopter that is already strengthened, such as the landing gear box for example.

In addition to structural and aerodynamic concerns, interference with helicopter subsystems preclude some choices for possible locations. This issue is strongly correlated to the kind of helicopter considered. Two possible mounting points for the Super Puma are examined, that could serve as examples of mounting sites for other aircraft.

In the Super Puma, the tail boom is composed of a double-box system (see figure below). The internal box is structural. Above it, different cowlings cover the tail rotor drive shaft. Since the tail rotor shaft is confined in a small cavity, there is no room to put the detector. Consequently the tail boom does not appear as a convenient site to place the detector.

Mounting points for the detector include: the engine sliding cowling and the landing gear

fairing (number 5 and 19 in the following figure)¹ as long as the depth of the detector box is not too high.

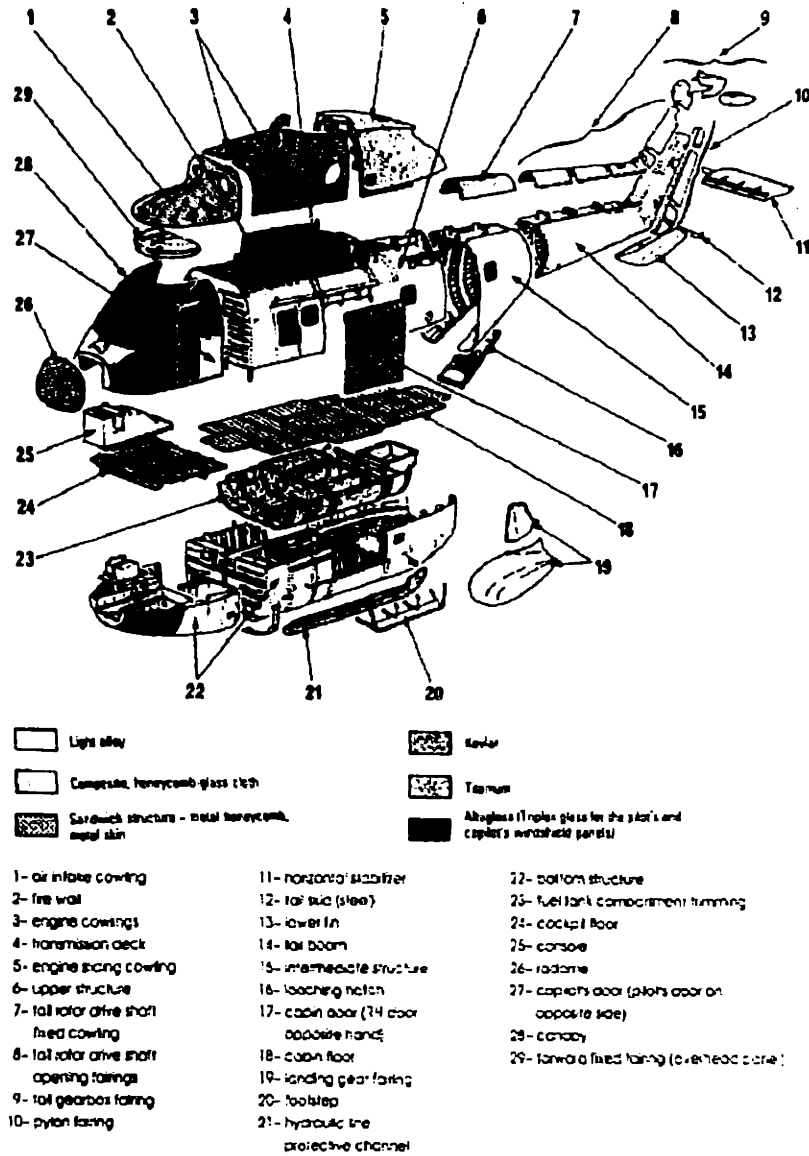


Figure 7-4: Exploded View of Eurocopter Super Puma

For the engine cowling location, the structure would have to be reinforced but this site is preferred because it is closer to all the flight systems and sources of power and therefore cables and wiring could be shorter. Besides, drag penalty on the landing gear box due to the presence of the detector could be more penalizing.

¹Courtesy of American Eurocopter.

7.5 Integration Cost

Regardless of which detector is used, the major cost does not come from the choice of one option versus another, but from certification.

Indeed, mounting one detector on a helicopter would probably require around 20 hours. Based on a work hour rate of one hundred dollars per hour, the cost of modifying the helicopter to put the detector would be about \$2,000. If everything is accounted for: implementation, wiring and aviation regulation authorities approval for non hazardous setup, the total cost would range from \$3,000 to \$5,000. This is the minimum cost to modify a helicopter for experiments².

If a definitive integration on a helicopter were to be done, then, the costs would be much higher, because of certification requirements. In order to deliver the supplemental type certificate needed for any modification, however minor, on the helicopter, aviation authorities would have to approve all the setup, wiring, power supply and the interfaces with the crew, let alone the functionality of the device. Though no precise estimate could be obtained at this point, it seemed that the cost of this process is several orders of magnitude higher than the cost of modifying the aircraft structure.

7.6 Comparison of Concepts

Three concepts have been considered so far, that have to be compared. Functionality and performance are not criteria for selection. Here, the three solutions have been assumed to meet the functional and performance requirements. If this were not the case for one candidate, i.e. if one optical protection option significantly compromised the signal, it would be automatically eliminated. The problem here is that no simple model allows for the estimation of the effects of a heated window/mirror on the path of the beam in terms of modification of the original signal. Therefore experiments should be useful to evaluate these effects³.

Assuming the same functionality for each of the concepts, criteria retained for comparison are: complexity, risk, power requirements and maintainability. The following table compares

²Estimates provided by George Sparling from American Eurocopter.

³Effects of blowing hot air onto a window were tested. See Chapter 5.

the different topics on this basis. As discussed in the previous section, cost is not really an issue but it will be introduced for additional information.

Criterion	Bleed Air Concept	Gold Grid	Heated Mirror
COMPLEXITY	<ul style="list-style-type: none"> • interdependencies with helicopter engine (fuel consumption increased resulting in power limitations) • requires subsystem to determine aperture of valve • need for additional ducts (adds mechanical complexity and serviceability is more difficult) • direct the flow onto the window => need for accurate deflectors 	<ul style="list-style-type: none"> • heating subsystem requires 2 grids separated by EMI shield insulator, can be bought "off-the-shelf" • electrical power is necessary for window 	<ul style="list-style-type: none"> • mechanical setup: vibration reduction, alignment, adjustable angle • water evacuation hole required => additional ducts • electrical power required through strip
POWER REQUIREMENTS	<ul style="list-style-type: none"> • related to electrical power supply and fuel consumption 	<ul style="list-style-type: none"> • voltage on grid, power supply for thermocouple 	<ul style="list-style-type: none"> • heat of the strip on the back of the mirror
SERVICEABILITY	<ul style="list-style-type: none"> • three levels: detector, ducts (mechanical links to compressor), compressor • simple subsystems • requires cleaning (before take-off) 	<ul style="list-style-type: none"> • detector set is a box (modular) => easy to maintain • requires cleaning (before take-off) 	<ul style="list-style-type: none"> • mirror subsystem more complex to handle
RISK	<ul style="list-style-type: none"> • proved technology (in inlet de-icing) 	<ul style="list-style-type: none"> • subsystems = replaceable or very difficult to repair due to innovative technology 	<ul style="list-style-type: none"> • not innovative
COST	<ul style="list-style-type: none"> • window: \$400 • ducts: depending on length (hence on position of box on helicopter) • valves and mechanical setup devices required 	<ul style="list-style-type: none"> • gold grid: minimum of \$20/part to mount the grid (based on 1,000 parts/year) • window (based on ZnSe) = \$400 	<ul style="list-style-type: none"> • mirror: \$150 • heating blanket: \$30

Figure 7-5: Comparison Matrix

Based on this table, the different options can be ranked for each criterion. This is presented in the next table.

Criterion	Bleed Air Concept	Gold Grid	Heated Mirror
COMPLEXITY • overall • subsystems	2+ 1	1 3	1 2
POWER REQUIREMENTS	1 engine compressor	2 electrical	2 electrical
SERVICEABILITY	2	1+ modular	3
RISK	1	3	2
COST	1 window ducts	1+ window grid	1 mirror blanket

Figure 7-6: Concept Ranking

These comparisons show that:

- The mirror system box seems the most complex. It also requires a larger area in the helicopter and needs very special care. Evacuation of water due to rain/melting snow is also difficult to implement. Holes on the bottom of the box should do the work provided the water does not damage the subsystems below. Moreover, vibrations might be critical for the mirror performance. However, the heating system is straightforward to implement and unexpensive. In addition, this option offers the best decorrelation between the protection

system and the detector box.

- The gold grid system seems attractive for its modularity and its simple implementation. Normally, as in engine inlet deicing, bleed air systems are preferred to electrical heating, because electrical power requirements would result in significant additional weight. Here, the area to be heated is small enough, and therefore, this may not be an issue. However, using the gold grid system introduces complexity in the window subsystem. In this case, complexity amounts to risk since the technology to implement a mesh on a Zinc Sulphide window has to be developed. Though some estimate costs have been given in the Comparison Matrix, technology risks translate into probable higher costs.
- The bleed air concept seems satisfactory in terms of risk and complexity, since this technology is already used for other heating applications. However, interfaces between the detector box ducts and the engine might require some mechanical work to set the connections with the engine: plumbings, valves conditioning the air flow, etc...

With this information, none of the concepts stands out as the best one. Moreover, a concept selection might also depend on the type of helicopter used. The bleed air solution, for example, is not well suited if the detector is to be mounted far from the engines, in which case, the length of the ducts and tubes would be deterrent.

Further steps for a concept downselection include:

- Laboratory (of field experiments if possible) to check the functionality and performance of each concept;
- Getting more information on the gold grid system by sending a request for quotation to possible suppliers, including all the characteristics of the system. This would make it possible to get more realistic estimates in terms of cost and complexity.
- Consulting helicopter manufacturers, both to determine mounting locations for the detector, and to learn about their preferences in terms of establishing interfaces between the detector and the helicopter subsystems.

Chapter 8

Conclusions and Recommendations

This work was intended to discuss two main issues related to the design of a prototype for an infrared ice detector for rotorblades: market assessment and design. From studying the possible market for the detector, it appeared that several kinds of helicopters could actually benefit from a blade ice detection capability, more precisely IFR certified medium size helicopters would be the best candidates to implement the detector. Moreover, field experiments and the requirement for a robust, all-weather operation detector brought to the fore the need for an optical protection system to prevent the optics from icing up. This led to the design of three possible protective systems: a gold grid heated window, a bleed air heated window and a heated mirror. Based on the information gathered, and considering Eurocopter Super Puma as the target helicopter, a comparison of the three options was proposed and further steps for a downselection were suggested.

Three different types of work have nourished this project: market studies, experimental work and design. It seems important to analyze what lessons have been learned and what recommendations could be made. Some of them may be obvious, but experience shows that reality is often beyond expectations.

First, market assessment studies showed the importance of asking the right questions to possible customers. For example, the detector had no real market intended for ice certified helicopters. The market analysis could have been limited but for MIT faculty suggesting another approach.

Secondly, lab and field experiments have revealed the difficulty to successfully test a theory even when experienced people are involved. This is not a big discovery, but the time it takes to fix some details and the number of unexpected problems arising in field experiments are important enough to mention. In this domain, considering the worst case should be a rule, because not all experiments can be repeated at will without serious consequences in terms of cost and time drifts. A successful experiment (specially field experiment) is not improvised and should be thoroughly prepared.

Finally, the design effort led to the more instructive conclusions. It should be noted that all the subjects discussed in this report and all the choices made are based on the knowledge and the information accessible during the four months of work. Some choices might have been different if more information had been available or consulted in further detail. The validity of some statements is therefore limited, but so is the validity of any choice made under time constraints. Apart from researchers maybe, this is the case of most decisions taken by engineers¹.

¹In this aspect, the guidance provided by MIT faculty (C. Boppe and Pf. Hansman) was really helpful.

Bibliography

- [1] Adam Dershowitz. *A Passive Infrared Ice Detection Technique for Helicopter Applications*. Thesis, MIT, 1991.
- [2] R.J. Hansman and A. Dershowitz. *Experimental Investigation of Passive Infrared Ice Detection for Helicopter Applications*. AIAA-91-0667, AIAA 29th Aerospace Sciences Meeting, January 1991.
- [3] R.J. Rieder. *A Low Cost Passive Infrared Sensor For The Remote Detection Of Ice*. Scientific Report , Visidyne, 1996.
- [4] R.J.Rieder. *Characterization of Room Temperature Pyroelectric Detectors*. Scientific Report N0.1, Visidyne VI-2752.
- [5] S. Krishnaswamy. *Comparison of HgCdTe, PbSe and Pyroelectric Detectors*. Report, Visidyne, 1996.
- [6] C. Boppe. *Aerospace Product Design*. Notes for 16.870, Massachusetts Institute of Technology, 1996.
- [7] Mikael A. Bramson. *Infrared Radiation A Handbook for Applications*. Plenum Press, New-York, 1968.
- [8] R.A. Smith, F.E. Jones and R.P. Chasmar. *The Detection and Measurement of Infrared Radiation*. Oxford at the Clarendon Press, 1960.
- [9] J. Wilson and J.F.B. Hawkes. *Optoelectronics, an introduction*. Prentice/Hall International, 1983.

- [10] Glenn R. Elion and Herbert A. Elion. *Electro-Optics Handbook*. Marcel Dekker, Inc. New York, 1979.
- [11] *Electro-Optics Handbook*. RCA/Commercial Engineering, Harrison, NJ, 1974.
- [KOK] Valentina F. Kokorina. *Glasses for Infrared Optics*. CRC Press, Inc., Boca Raton, FL., 1996.
- [12] J.A. Savage. *Infrared Optical Materials and their Antireflection Coatings*. Adam Hilger Ltd., Bristol, England, 1985.
- [13] *Briefs*. National Transportation Safety Board, 1997.
- [14] *Utilization of Infrared Detectors*. Proceedings of the Society of Photo-Optical Engineers, vol. 132, Los Angeles, CA, 1978.
- [15] *Infrared and Optical Transmitting Materials*. Proceedings of SPIE-The International Society for Optical Engineering, vol. 683, San Diego, CA, 1986.
- [16] *Optical Engineering for Cold Environments*. Proceedings of SPIE-The International Society for Optical Engineering, vol. 414, Arlington, VA, 1983.
- [17] *Optics in Adverse Environments*. Proceedings of the Society of Photo-Optical Engineers, vol. 121, San Diego, CA, 1977.

Appendix A

Chronology of the Project

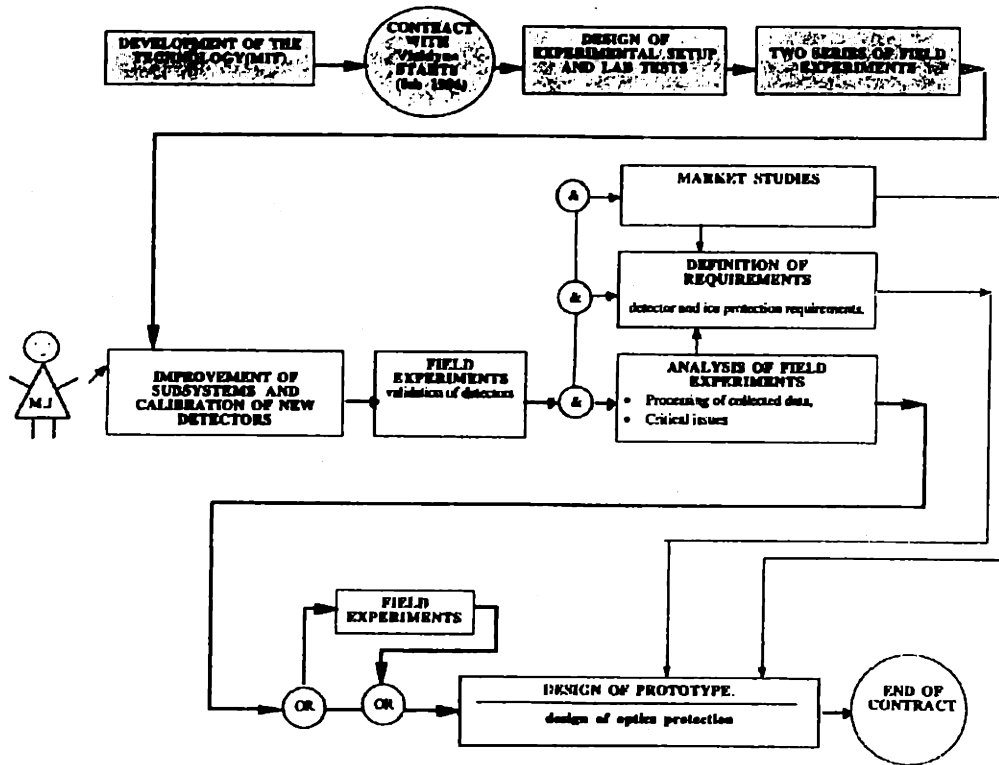


Figure A-1: Chronology of the Project

Appendix B

Blackbody Radiation

Some characteristic curves of the power emitted by a blackbody as a function of temperature and wavelength are shown in the following plots.

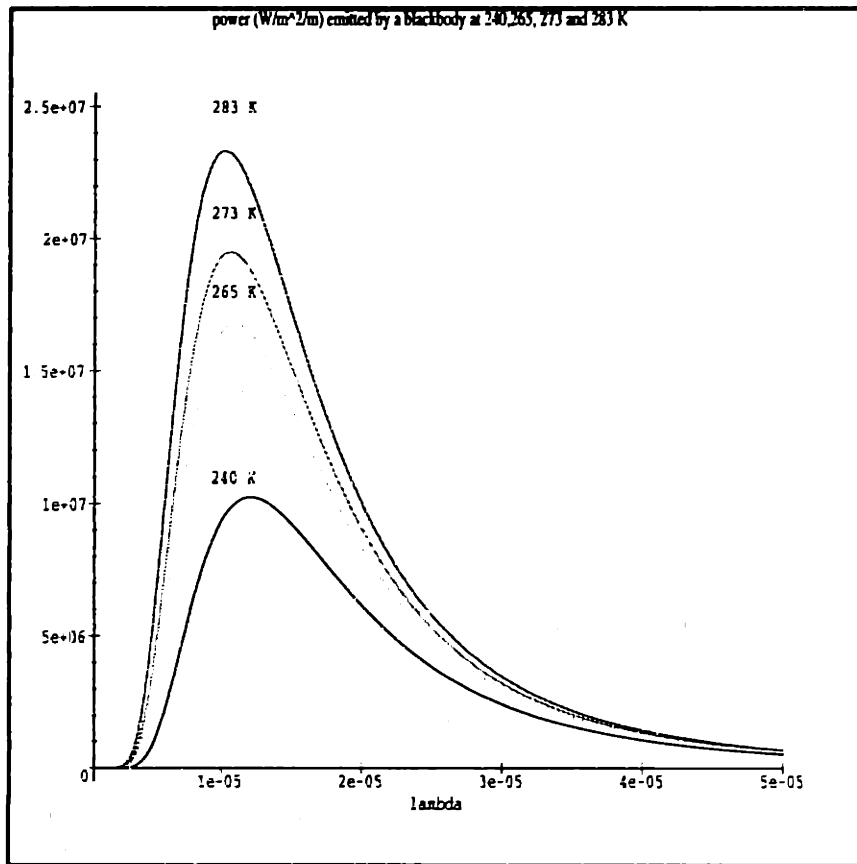


Figure B-1: Typical Blackbody Radiation Curves at Different Temperatures

Appendix C

Acronyms

- DGA: Délégation Générale pour l'Armement, French governmental organization in charge of Armament programs
- DGAC: Direction Générale de l'Aviation Civile
- FAA: Federal Aviation Administration
- FAR: Federal Aviation Regulations
- IFR: Instrument Flight Rules (see VFR)
- MCT: Mercury Cadmium Telluride (detector)
- NTSB: National Transportation Safety Board
- QFD: Quality Function Deployment
- PbSe: Lead Selenide (detector)
- rms: root mean square
- SNR: Signal-to-Noise Ratio
- VFR: Visual Flight Rules

Appendix D

Summary of Interviews

In the "Market Assessment" chapter, the analysis proposed is based on a synthesis of the information obtained from different people at various companies or organizations. Sometimes, opinions were slightly discrepant and it may be interesting if not revealing to get an idea of who thinks what ¹. In the following sections, a brief summary of the interviews with each contact, is provided based mainly on the answer to the questions (modulated for each contact) :

- How many accidents involving (your) helicopters have been caused by icing ?
- How useful would a remote ice detector for blades be ? Would you buy this product ? Why and how many (if applicable) ?
- What would you expect of such a product ? What would you require ? What constraints would you impose?

For the governmental organizations, the questions were different since they have been centered on the scope of their activities. This includes the Délégation Générale pour l'Armement and the Federal Aviation Administration.

¹Again, I am grateful to all the people that helped me, and I hope to be faithful to the message they passed on

D.1 Organizations

D.1.1 Délégation Générale pour l'Armement

(contacts: Luc Renouil, assistant manager helicopter division, J.J. Nobili, responsible of qualification problems, M. Corlay, responsible of the icing division) It seems though that detection of blade icing is critical for the helicopter performance, especially on thin profiles. Ice detection/protection devices are not valuable, however, if the aircraft has no adapted navigation/visualization system to fly under the severe conditions imposed by icing. In France, even if some work is done to protect medium size helicopters such as the Ecureuil or the Dauphin (Eurocopter), Eurocopter does not seem to be willing to deal with rotor qualification. Indeed, one major issue in this domain is certification, whose cost is dramatic². Several factors account for this high cost : stringent regulations, difficulty in finding the right icing conditions for the tests, difficulty in modeling the effects of icing, which increases the number of tests. In France and the United States, there is no limiting icing certification as in Great Britain or other countries. Consequently, either the aircraft is fully certified at a very high cost, or it is not certified and should not take-off if icing is a risk. For those countries that allow limited-icing certifications, helicopters equipped with ice detectors for blades might be worthwhile. In addition, Armed Forces, who have very high requirements for all-weather are possible "good" customers. The French Army, for example, has 24 certified aircraft.

D.1.2 Federal Aviation Administration

(contact: Lens Grant, helicopter certification division)

The United States has the same kind of regulation for icing certification for helicopters and airplanes but this process is very rare for helicopters : 2 certifications in 10-15 years. Before the process is launched, a hundred hours of flight testing are required. Then evidence has to be shown that the aircraft meets Title 14 Federal Aviation Regulations part 27 and 29 for normal category certification as well as Appendix C.

²DGA, in charge of the Flight Test Center, has conducted the testing for the certification of the Super Puma-Mark 1 in association with Eurocopter. Note of the author

D.2 Manufacturers

D.2.1 Eurocopter France

(contact: Mrs. Anne-Marie Cazin, assistant manager of the Icing Department)

Since blade icing can be noticed quickly from the vibrations, a detector is not really necessary. Remote ice detection could be valuable to look at the clouds instead. Eurocopter develops the only helicopter in the world to fly under unlimited icing conditions. Besides European armies will be equipped with an ice-protected helicopter as well: NH90³. If the aircraft is to be certified, the major issue is to evaluate the proportions of ice protections, which amounts to determining the power to apply, the residual frost on the blade and the degradation of performance.

D.2.2 American Eurocopter

(contact: Bill Force, Chief Test Pilot)

In the United States, no helicopter is certified to fly under icing conditions⁴. This implies that accidents due to icing are limited because if an aircraft is not certified, it should not take-off. Moreover, the main problem in terms of icing lies on engine intakes and not in the blades because their composite structure allows to shed ice very well. Consequently, the market for an ice detector should be limited in the United States. An estimated hundred aircraft could possibly be equipped with a remote ice detector. In fact, there might be major opportunities in northern countries. Operators required to fly frequently under IFR conditions should be interested in that kind of detector. This includes: medical evacuation services, corporate executives, off-shore operators, especially in the North Sea, where they have the ability to fly under icing conditions. In any case, top requirements for this detector are : low weight, especially if it were to be mounted in the tail boom of an helicopter where momentbalance is crucial, and reliability. Such a product is valuable only if it is coupled to a system that allows to get rid of the ice.

³Under development

⁴Note that only one Super Puma has been sold in the United Stated to Donald Trump. Note of Bill Force.

D.2.3 Sikorsky

(contact: Richard Fleming)

In terms of regulation for flight under icing conditions, there is a significant difference between certification and qualification. One helicopter in the world is certified for icing conditions: the Super Puma (Eurocopter). This certification is delivered by governmental agencies in charge of flight regulations: FAA (US), DGAC (France), CAA (Great Britain). Even if a helicopter is not certified, it can be qualified by the Army for operations under severe conditions. This is the case of Sikorsky's Blackhawk that is qualified for a flight envelope not as stringent as it would be for certification. This helicopter is equipped with a temperature sensor on the windshield and an airframe ice detector on the side of the engine. What happens on the blade is inferred based on the information from these devices.

In fact, Sikorsky has equipped several of their helicopters with airframe-type detectors. None of them was certified (though the Blackhawk or S76 almost was) for economic reasons. Certification can take years and is very expensive for an uncertain result: Super Puma sales were not overwhelming. Moreover, potential customers interested in having icing certified helicopters are reluctant to pay the cost of certification, and obviously so is the manufacturer. However, non certified aircraft equipped with ice detectors are valuable for some specific customers. R. Fleming indicated the following possible customers: the Army/Navy (US, Australia, Japan), Corporate executives , Emergency Services, Off-Shore Operators (maybe a limited market), Commercial Transport. If the ice detector for blades were available, Sikorsky (who is conducting a study in association with Boeing and Bell Heli Textron to determine what is the best ice detector/protection device in the market) might consider implementing it on their medium/large size helicopters: EH 101, S76, Blackhawk (military version), CH 53E Super Stallion, S92 and maybe the Commanche. The main requirements would then be: low weight, low initial cost, high reliability/accuracy; low direct operating cost. Military customers might also require low radar reflectivity. Nevertheless, such a detector is not worthwhile if not coupled to an ice removing system.

D.2.4 McDonnell Douglas

(contact: Richard Lee, test pilot)

Regarding icing, blades and engines are two major problems. Of course, light ice can be shed by the blade, but in a severe icing environment this might not be true. For large helicopters, though the resistance to ice is better and they can carry ice without really noticing. In fact, a remote detector for blade icing can be valuable for increasingly IFR certified helicopters. Two models of McDonnell Douglas series could be equipped with this kind of detector: MD 900 Explorer and Apache widely used for military applications. Weight would be a major constraint: 2 to 5 pounds are acceptable for this application. Aerodynamic cleanliness would also be a major requirement. Potential buyers would be the Military, aeromedical services and law enforcement organizations. Large utilizations of the ice detector can be expected in icy regions as in Europe.

D.2.5 Boeing

(contact : Andy Peterson)

Helicopters manufactured by Boeing are used for military applications, for which no accident due to icing was reported. Regarding blade icing, the difference between long, thick blades and smaller thinner ones is dramatic. Accretion efficiency is critical for small blades resulting in a degradation of performance in about two minutes. For larger blades, it can take up to thirty minutes before the consequences of ice are noticeable. The value of an ice detector for ice protected helicopters lies on the power margin it permits, since it allows to switch on the heating devices when there is evidence of ice. Boeing might consider implementing the ice detector for blades on : the Commanche, Chinook, V22 (26) provided it is effective, not expensive, light and has low EMI signature.

D.2.6 Bell Helicopters

(contact: Tom Warren, test pilot)

An ice detector for blades is likely to be valuable in the coming years provided it can list the amount of ice and it is associated with an ice removal system. However the need seems mild.

D.3 Services

Unfortunately, the information on this section is limited to one helicopter operator. Other services were contacted, but no useful information was obtained.

D.3.1 Era Services-Alaska

(contact: Larry Schmidt, chief pilot)

The value of an ice detector seems clear. About 3 to 4 % of the flights are cancelled for icing reasons, on a basis of 100 flights per day. This company operates helicopters for different kinds of services: medical, charter, flight for oil companies. The latter is the more important of their market (about 60 %) and also the more critical in terms of flights in icing conditions. Their operations are worldwide: Alaska, Louisiana, China, the Netherlands, Great Britain and the North Sea. With a fleet of around 100 helicopters, composed of small Bell 206's, Eurocopter AS350 Astar, BK 105 and larger IFR certified Bell 212, Bell 412 and Super Pumas, about 32 % of their aircraft would be equipped profitably with an ice detector. Even if the helicopter were not certified, this would provide with a warning system that would allow the pilot to adopt an anti-ice strategy.

Appendix E

List of Contacts

The list of contacts is included in this appendix, divided by subjects of interest. Thanks to all the people who helped me in collecting information.

E.1 On general topics related to helicopter icing

- Marcia Politovitch, *National Center for Atmospheric Research*, 1 (303) 497 8449.
- Latricia Carter, *National Transportation and Safety Board*, 1 800 877 6799 (ext. 6550).
- Lens Grant, *Federal Aviation Administration*, 1 (817) 222 5114.
- R. Berger, *US Army Cold Regions Research and Engineering Lab*, 1 (603) 646 4361.
- Mario Vargas, *Nasa Lewis Research Center*, 1 (216) 433 2064.
- Luc Renouil, J.J. Nobili, M. Corlay, *Délégation Générale pour l'Armement (France)*, 011 33 1 45 52 42 55.

E.2 On market possibilities

- Bill Force, *American Eurocopter*, 1 (972) 641 3550.
- Mrs.Cazin, Mrs. Nuques, *Eurocopter France*, 011 33 42 85 (85 73)/(87 57).

- Richard Fleming, *Sikorsky*, 1 (203) 386 4000.
- Richard Lee, *McDonnell Douglas*, 1 (602) 891 3000.
- Andy Peterson, *Boeing Helicopters*, 1 (610) 591 2675.
- Larry Schmidt, *Era Services*, 1 (907) 248 4422.

E.3 On the protective device

- Lew Herczeg, *Army*, 1 (201) 724 6272.
- Jack Walf, *Evaporated Coating*, 1 (215) 659 3080.
- Mark Michell, *General Dynamics Land Systems*, 1 (810) 825 5755.
- Greg Rapp, Dave Criane, *Litton Electro-Optical Systems*, 1 (214) 342 5161 .
- Bill Hermann, *independent consultant*, ¹ 1 (214) 270 36 01.
- George Sparling, *American Eurocopter*, 1 (972) 641 3554.

¹formerly responsible for the design of gold grids

Appendix F

Experimental Investigation of Passive Infrared Ice Detection for Helicopter Applications

This appendix gives a reproduction of the paper presented at the 29th Aerospace Sciences Meeting (January 1991, Reno, NV) by A. Dershowitz, Research Assistant and R.J. Hansman, Professor at MIT ([2]), in which the theory of remote ice detection for rotorblades is explained.



AIAA-91-0667
**Experimental Investigation of Passive
Infrared Ice Detection for Helicopter
Applications**

A. Dershowitz and R.J. Hansman
Dept. of Aeronautics and Astronautics
Massachusetts Institute of Technology
Cambridge, MA

29th Aerospace Sciences Meeting
January 7-10, 1991/Reno, Nevada

For permission to copy or republish, contact the American Institute of Aeronautics and Astronautics
370 L'Enfant Promenade, S.W., Washington, D.C. 20024

Experimental Investigation of Passive Infrared Ice Detection for Helicopter Applications

Adam Dershowitz* and R. John Hansman, Jr.**
Department of Aeronautics and Astronautics
Massachusetts Institute of Technology
Cambridge, Massachusetts U.S.A

Abstract

A technique is proposed to remotely detect rotor icing on helicopters. Using passive infrared (IR) thermometry it is possible to detect the warming caused by latent heat released as supercooled water freezes. During icing, the ice accretion region on the blade leading edge will be warmer than the uniced trailing edge resulting in a chordwise temperature profile characteristic of icing. Preliminary tests were conducted on a static model in the NASA Icing Research Tunnel for a variety of wet (glaze) and dry (rime) ice conditions. The characteristic chordwise temperature profiles were observed with an IR thermal video system and confirmed with thermocouple measurements. A prototype detector system was built consisting of a single point IR pyrometer, and experiments were run on a small scale rotor model. Again the characteristic chordwise temperature profiles were observed during icing, and the IR system was able to remotely detect icing. Based on the static and subscale rotor tests the passive IR technique is promising for rotor ice detection.

1. Introduction

The reliable measurement of ice accretion is an important requirement for helicopter all-weather operation. Rotor icing can present a significant hazard due to increased torque requirements, aerodynamic performance degradation, control problems and severe vibrations resulting from uneven ice shedding. Helicopter exposure to icing conditions has increased over the past decade due to the increase in routine instrument flight operations.

* Research Assistant

** Associate Professor, Associate Fellow AIAA

Copyright © 1991 by M.I.T. Published by the American Institute of Aeronautics and Astronautics, Inc. with permission.

The two primary helicopter applications for ice detection are the monitoring of critical components for Caution and Warning alerts, and the management of ice protection systems. For Caution and Warning applications, ice accretion on critical components should be detected before a hazardous condition exists.

Because rotating components often experience a significantly different icing condition than the fuselage, visual evidence of ice accretion on non-rotating structures is not adequate for Caution and Warning applications. Indirect indications of icing such as torque rise or vibration typically emerge only after the hazardous condition exists. Ideally, the direct measurement of ice accretion on the rotating components would provide the earliest and most accurate measurement of potential icing hazards.

For helicopters equipped with ice protection systems, the management of these systems can be critical. The most common type of rotor protection is electrothermal deicing. These systems require significant amounts of electrical power so the blades are typically deiced in segments. Because there are no effective rotor ice detection systems it is necessary to overheat and continually cycle the electrothermal deicing systems to assure adequate ice protection. If effective ice detection were employed the deicing systems could be operated more efficiently and effectively.

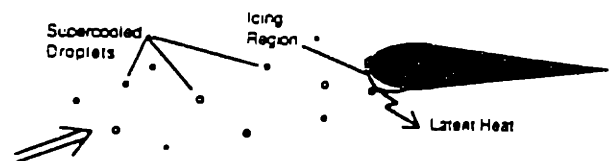


Fig. 1 Schematic representation of latent heat release during icing

2. Background

2.1 Existing Ice Detection Techniques

The most common ice detectors currently employed for aviation applications are direct contact type devices. In contact type detectors, either a probe or surface mounted transducer senses the ice presence through a variety of physical mechanisms. These include resonant frequency shifts, optical blocking, heat capacity, electrical capacity, and ultrasonic thickness gauging.¹

Contact type ice detectors have not been successfully utilized for direct measurement of rotor ice accretion due to the difficulties inherent in instrumenting the rotors. These include mounting restrictions imposed by structural limitations of the blade, transmission of information between the rotating and non-rotating frames, acceleration limitations of the sensors, and erosion problems. As a result, contact type detectors are typically mounted on the fuselage and the rotor conditions are inferred.² These techniques have had limited success because of the complex dependence of the icing process on temperature, liquid water content and velocity, which vary significantly between the fuselage, and rotor as well as along the blade span itself.

2.2 Remote Monitoring of Rotating Blades

Remote sensing offers significant advantages for monitoring rotating blades. If ice accretion can be remotely detected by sensors mounted in the fuselage, then a direct measurement of rotor ice accretion can be accomplished without the difficulties identified above. Several potential techniques have been investigated for remote ice detection including: high speed video, and active microwave. The technique which has emerged as the most promising is passive infrared.

3. Passive Infrared Ice Detection

3.1 Theory of Operation

The passive IR technique detects ice accretion through remote IR thermometry of the icing surface. When ice accretes on an airfoil or rotor, the region where the accretion occurs becomes warmer than the surrounding surface due to release of the latent heat of fusion as the impinging supercooled water droplets freeze. This process is shown schematically in Fig. 1. It should be noted that the ice accretion is typically limited to a small region near the leading edge, and that much of the rotor surface will remain clear of ice. These uniced areas will have surface temperatures at or near the ambient temperature which will always be below freezing in icing conditions.

As a result of the thermodynamic processes described above, the rotors will exhibit a characteristic chordwise surface temperature profile when in icing conditions. Schematic temperature profiles are shown in Fig. 2 for wet and dry icing conditions. Prior to icing, the rotors will equilibrate to some temperature slightly warmer than the static air temperature due to kinetic heating. During icing, the temperature will increase in the accretion region as indicated in Fig. 2. For wet (glaze) ice accretions, the wet stagnation region will remain at 0°C while for dry (rime) accretions the temperature will reach a peak in the stagnation region at some temperature below freezing.

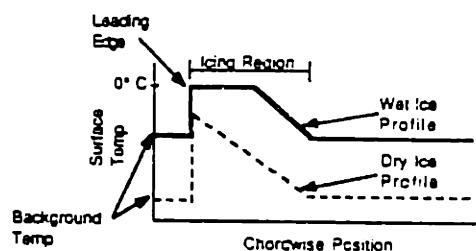


Fig. 2. Schematic chordwise temperature profiles for wet and dry icing conditions

In the proposed technique, shown in Fig. 3, the rotor surface temperature would be measured by an infrared pyrometer mounted on the fuselage which scans the blade in the chordwise direction as it passes overhead. The aim point of such a detector could be varied between spanwise positions to give full coverage of the blade. Infrared pyrometers are commonly used to remotely measure surface temperature through thermally emitted black body radiation in the IR spectrum.

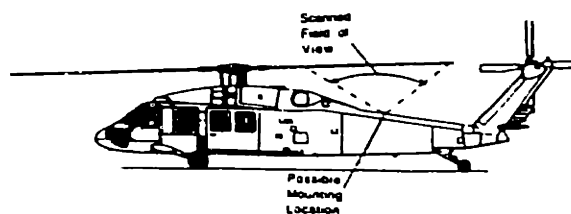


Fig. 3. Possible helicopter mounting scheme for a passive infrared ice detector

Passive IR video thermography has been used for several years in the U.S. and France as a diagnostic tool for validation of ice accretion modeling codes.^{3,4} Synchronized IR video images have also been used to monitor rotating components in flight as part of the Advanced Turboprop development effort.⁵ Due to uncertainty in surface emissivity, attenuation through the icing cloud and thermal drift of the detectors it is

sometimes difficult to accurately measure absolute temperature, however relative temperature resolution of 0.2°C is achievable. This is considered adequate for ice detection where only the relative temperature profile between the leading and trailing edge regions is required.

The passive IR system also has the potential to be used to monitor the operation of thermal deicing systems. Once ice sheds, the relatively hot blade surface will be exposed, resulting in an identifiable thermal signature.

3.2. Static Tests

3.2.1 Experimental Setup for Static Tests

In order to evaluate the feasibility of the passive IR ice detection concept, a series of static tests were conducted in the NASA Icing Research Tunnel (IRT). These preliminary tests were conducted on a non-rotating 6 ft. chord airfoil model with a 25° sweep which could be varied between $\pm 20^{\circ}$ angle of attack. The model was instrumented with thermocouples and electrothermal heaters in the leading edge region.

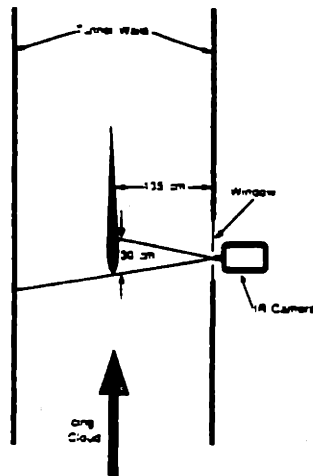
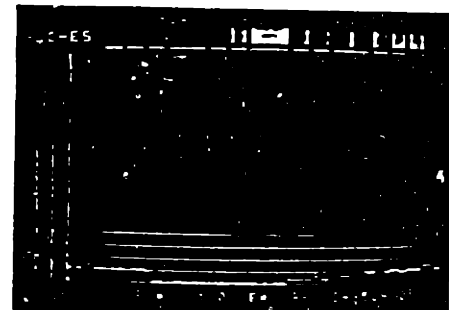


Fig. 4. Schematic of IRT setup

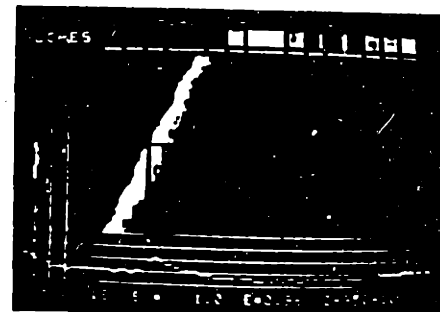
Infrared diagnostics were provided by a Hughes Probeye thermal imaging system which uses 6 Indium Antimonide (InSb) detectors and a spinning mirror to scan both horizontally and vertically. This imaging system, while somewhat more complex than required for an ice detection system, employs IR detectors very similar to those proposed for use in the passive system. These detectors, when cryogenically cooled, are sensitive in wavelengths from 2.0 to 5.6 microns. In the imaging system the output of the detectors was fed into a processor that developed thermal video images and chordwise temperature profiles. The data was stored on

videotape. In the experimental set up, shown in Fig. 4, the IR camera was mounted outside of the tunnel and viewed the leading 30 cm of the airfoil through a hole in the tunnel window.

Experiments were run over a wide range of icing conditions, with airspeeds from 208 mph (93 m/s) to 129 mph (58 m/s) temperatures from -17°C (2.4°F) to -3°C (26°F) and liquid water content (LWC) from 0.53 g/m^3 to 1.96 g/m^3 . For each experimental run the airfoil was first cleared of any ice. The airspeed and temperature of the wind tunnel was stabilized and the spray was then turned on for a predetermined time span, typically 1 to 3 minutes. In some cases the spray was cycled on a second time, for 30 seconds, without deicing first. This second cycle allowed verification of the ability of the technique to detect ice accretion over an existing ice layer.



IRT ICING CLOUD OFF



IRT ICING CLOUD ON
(NOTE WARMING OF LEADING EDGE)

Fig. 5. IR video output of model lower surface
($T = -11^{\circ}\text{C}$, $V = 92\text{ m/s}$,
 $\text{LWC} = 0.17\text{ g/m}^3$)

3.2.2. Static Test Results

A typical IR video image is presented in Fig. 5 for the swept airfoil at a tunnel temperature of -11°C , a LWC of 0.17 g/m^3 , with a mean volumetric diameter (MVD) of approximately 15 microns, an angle of attack

of 4°, and a free stream velocity of 92 m/sec. Note that the chordwise temperature profile is shown across the bottom of the image. With the spray off, the airfoil surface temperature is uniform at approximately the tunnel temperature. When the spray is turned on, the increase in leading edge surface temperature resulting from the latent heat release is clearly visible. After the spray was turned off, the leading edge would slowly cool as the remaining liquid water on the surface froze.

The IR and thermocouple measured chordwise temperature profiles for typical wet (glaze) ice conditions are presented in Fig. 6. In this case the tunnel temperature was -5°C, the LWC was 1.95 g/m³, with a MVD of 20 microns, the angle of attack was 10°, and the free stream velocity was 59 m/s. With the spray off, the airfoil had a uniform indicated temperature. The warmer temperature observed upstream of the stagnation point is an image of the warm tunnel wall behind the airfoil. When the spray was turned on, the expected surface temperature profile for wet growth was observed. The leading 8 cm of the airfoil indicated a surface temperature of 0°C indicating wet ice growth. Aft of the wet region, the surface temperature dropped to the uniced value. The IR measurements were consistent with the thermocouple readings. The LEWICE ice accretion code was run to simulate ice growth at these same conditions. The LEWICE predicted surface temperatures, as shown in Fig 7, are consistent with those measured with the

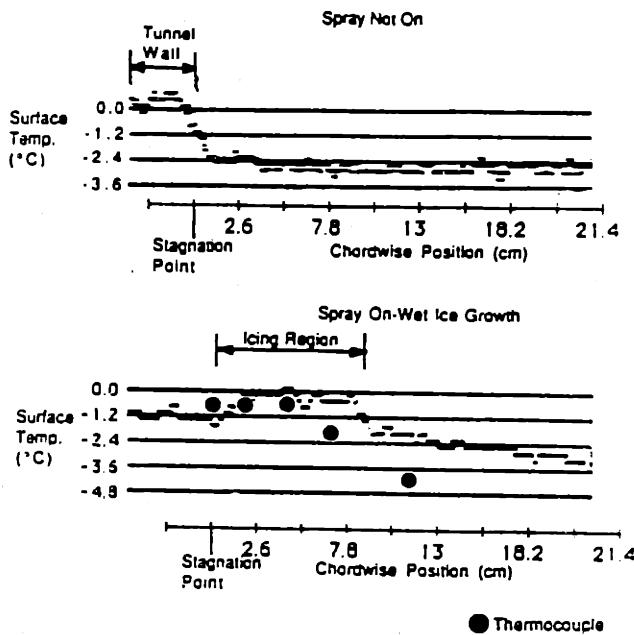


Fig. 6. Chordwise temperature profiles for wet (glaze) ice conditions ($T=-5^{\circ}\text{C}$, $V=59\text{m/s}$, $\text{LWC}=1.95\text{ g/m}^3$)

IR system. When the spray was turned off the surface temperature again became uniform as the surface water froze. When the spray was cycled on, the characteristic wet ice temperature profile was again observed.

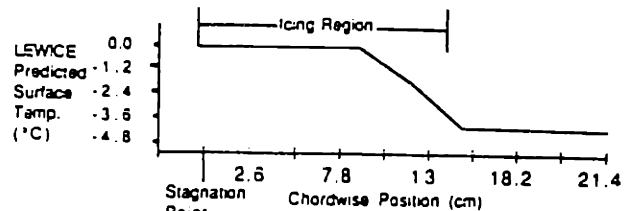


Fig. 7. LEWICE predicted temperature profile for wet (glaze) ice conditions ($T=-5^{\circ}\text{C}$, $V=59\text{m/s}$, $\text{LWC}=1.95\text{ g/m}^3$).

The IR measured temperature profiles for a dry (rime) ice condition also show the expected temperature profile. An example is presented in Fig. 8. In this case the tunnel temperature was -17°C, the LWC was 0.17 g/m³, with a MVD of approximately 15 microns, the free stream velocity was 92 m/s and the angle of attack was 4.1°. With the spray off, the airfoil had a uniform indicated temperature. When the spray was turned on, the surface temperature was seen to peak at the stagnation point. This curve is characteristic of dry (rime) growth where the surface temperature reflects the local collection efficiency (i.e. increased impingement causes increased icing and increased heating). The stagnation point has the largest collection efficiency and consequently the greatest latent heat release. When the spray was turned off the temperature quickly dropped to the preicing value. The characteristic rime ice profile again appeared when the spray was cycled on.

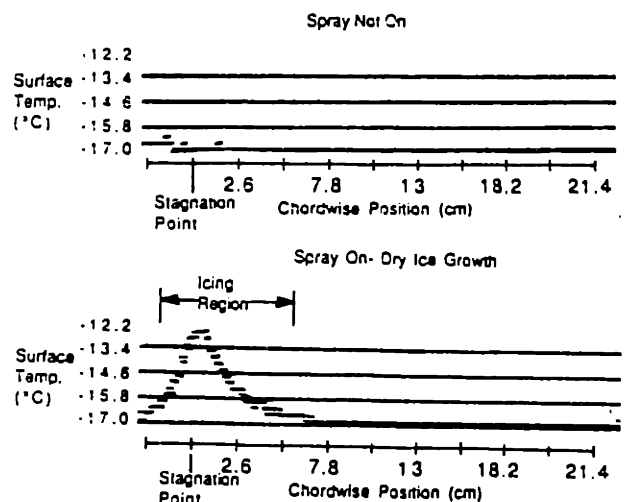


Fig. 8. Chordwise temperature profiles for dry (rime) ice conditions ($T=-17^{\circ}\text{C}$, $V=92\text{m/s}$, $\text{LWC}=0.17\text{ g/m}^3$).

3.3 Rotor Tests

3.3.1 Infrared Ice Detector Design

In order to evaluate the IR ice detection technique on rotating systems a prototype detector, suitable for both flight and ground tests, was developed. This ice detector, shown in Fig. 9, is essentially a point infrared pyrometer. It was built around a HgCdTe (Mercury Cadmium Telluride) infrared detector. This detector was chosen as it offers high sensitivity in the range of 2-5 microns, using only thermoelectric cooling. Other detector types were considered, as they offer higher sensitivity, or operate at longer wavelengths. However they require cryogenic cooling, which would not be practical for flight operations. This detector uses a four stage thermoelectric cooler, with an automatic controller, to keep the temperature of the detector at -73°C . A gel cell battery was used to provide the bias for the detector at 2.6 V.

The HgCdTe detector is positioned at the focus of a single Calcium Fluoride (CaF_2) lens. The simple biconvex lens had a 10 cm focal length. Calcium Fluoride was selected as it has high transmissivity in the necessary IR band and is not overly sensitive to thermal shock, or water degradation. Concentric aluminum tubes were used, with a Teflon sleeve, to allow the length of the pyrometer to be adjusted giving a focus for a target distance from 15 cm to infinity. This range allows the prototype to be used on a small test rotor or in full scale flight tests. This lens gave the detector a target spot size of 0.18 cm diameter at 56 cm as used in the tests, and a spot size of 1 cm diameter at 3 m, typical of a helicopter application. In order to prevent icing or fogging of the lens small gas jets were set up to spray dry nitrogen across the lens.

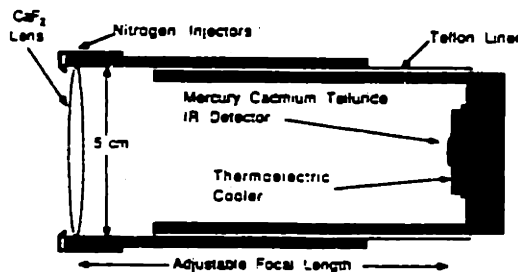


Fig. 9. Infrared ice detector schematic

The signal from the pyrometer itself was processed as shown in Fig. 10. It was first fed into a high gain, low noise amplifier. The amplifier was AC coupled to prevent saturation. This had the effect of amplifying only short term temperature changes. The signal was sent into a digital oscilloscope, and stored for post processing if required.

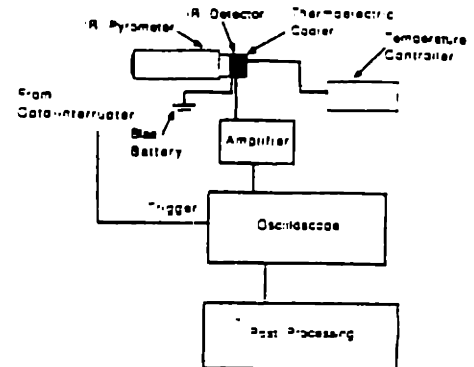


Fig. 10. Ice detector signal processing path

3.3.2. Test Rig For Rotating Tests

In order to test the prototype ice detector, a test rig was constructed. It consisted of a single blade counter-balanced rotor with a 22 cm span and a 2 cm chord, built of aluminum, schematically shown in Fig. 11. The small rotor was chosen to allow the entire rig to be placed in a lab freezer. This system was able to run over a wide range of rotation speeds, from 0 Hz to 40 Hz. The tests were nominally run at 22 Hz which allowed good ice formation, at reasonable rotor Reynolds numbers. The blade passed through the field of view of the pyrometer at an angular speed typical of a tail rotor, which is several times faster than that of a main rotor. This test therefore was conservative in that significantly faster detector dynamics were required than would be necessary for main rotor use. The angle of attack was adjustable over a range of positive and negative values. An opto-interrupter was set up across the blade to measure rotation rate and to provide trigger pulses for tracking the blade.

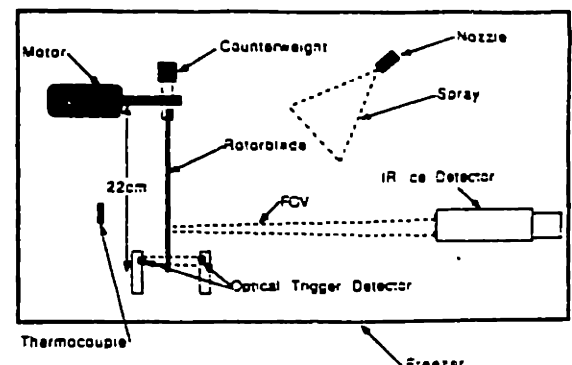


Fig. 11. Rotor test rig

The rotor and ice detector were both mounted in a freezer which had a minimum temperature of -23°C . The lens was 56 cm from the rotor plane. The ice detector was aimed at the 13.5 cm span position of the rotor, and focused to provide the sharpest signal possible. Because of the exploratory nature of the tests, an uncalibrated water spray was considered adequate. A simple spray system with an estimated LWC of 0.9 g/m^3 at the rotor was used. The freezer temperature was measured using a thermocouple.

3.3.3. Experimental Procedure

For a typical experimental run the blade rotation rate and freezer temperature were allowed to stabilize. The temperature and rotation rate were recorded. An uniced temperature profile was then recorded. Water at 0°C was then sprayed for 10 sec and a temperature profile during icing was recorded. Several profiles were recorded after the icing event while the blade temperature profile was returning to equilibrium. Again the temperature and rotation rate were recorded. Finally the blade was deiced and the cycle was repeated. These runs were done over a range of temperatures from -20°C to 60°C , and at several different angles of attack. During icing the rotation rate would drop slightly due to the increased drag from the ice, and the temperature would rise from opening the freezer, which was necessary to initiate the spray.

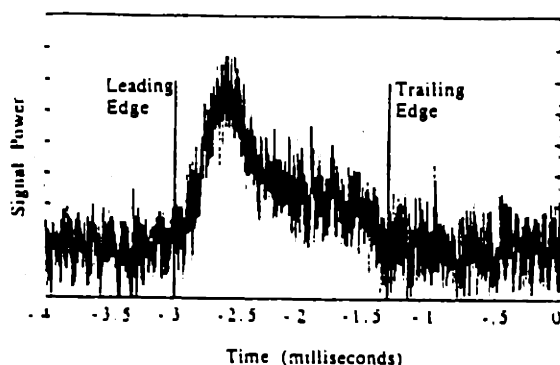


Fig. 12a. Unfiltered IR temperature profile

3.3.4. Rotor Results

A typical unfiltered signal from the pyrometer is shown in Fig. 12a at -6.8°C , 22 Hz and 0° angle of attack. The signal is shown in arbitrary units because only the temperature profile is of interest and the signal scales with amplifier gain, DC offset, and detector bias voltage. Because the signals contained a component of high frequency noise, they were digitally low pass filtered at 10 kHz resulting in signals as shown in Fig. 12b. As expected there was significant heating in

the leading edge region, where there was icing occurring, while the rest of the blade remained at a relatively constant temperature. This is the same characteristic profile that was measured in the static tests. Before the spray began, the blade and the back wall of the freezer were at thermal equilibrium as indicated by the relatively flat line.

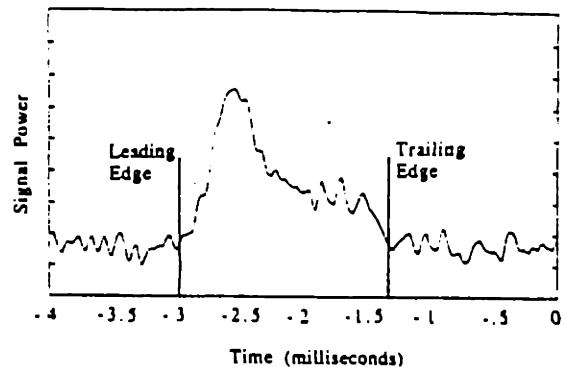


Fig. 12b. IR profile filtered at 10 kHz

Figs. 13 through 16 show the effect of ambient temperature on the signal. For all of these cases the rotor started at 22 Hz with 0° angle of attack, and the spray LWC is 0.9 g/m^3 . During very cold conditions, such as Fig. 13 (-15°C) where there was a large temperature difference between ambient and freezing, there was a correspondingly large temperature change in the icing (leading edge) region of the blade. This resulted in the strong temperature profile shown in Fig. 13. Fig. 14 (-6.8°C) show a signal typical of glaze ice, where the icing profile is clearly visible. Fig. 15 (-3°C) shows a case just below freezing, where there was minimal glaze ice. Because the ambient temperature was close to 0°C the signal is small but clearly detectable. When the blade was stopped to be deiced there was only a small amount of ice present. A temperature profile taken at a temperature just above icing conditions is shown in Fig. 16. There was no signal indicative of icing, which is consistent with the observation that there was no ice accretion on the blade after the run.

In order to evaluate any changes in detectability with angle of attack, the angle of attack was varied over several runs. There was very little change in the temperature profile signal, although the higher angle of attack runs did include a slightly wider heating region, due to the increased size of the icing region.

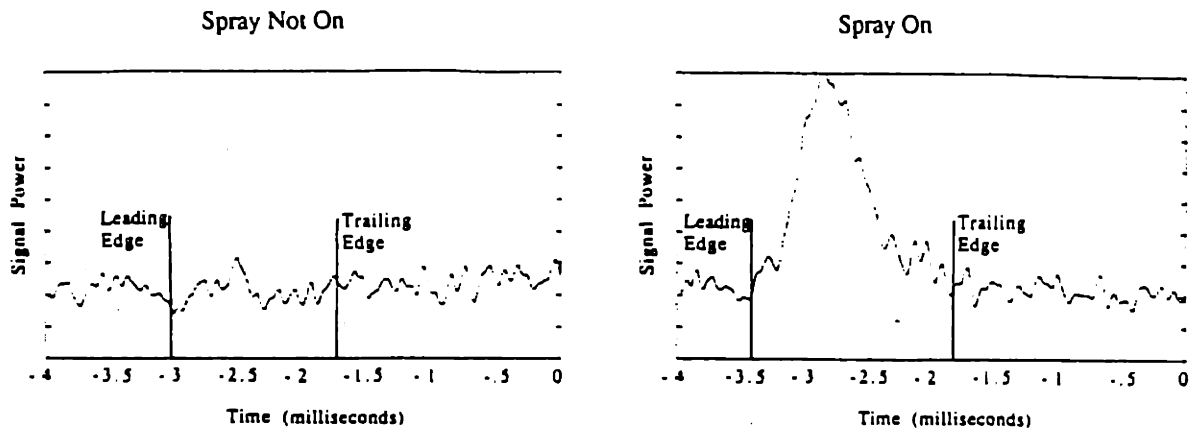


Fig. 13. IR Profiles at $T=-15^{\circ}\text{C}$ with and without water spray

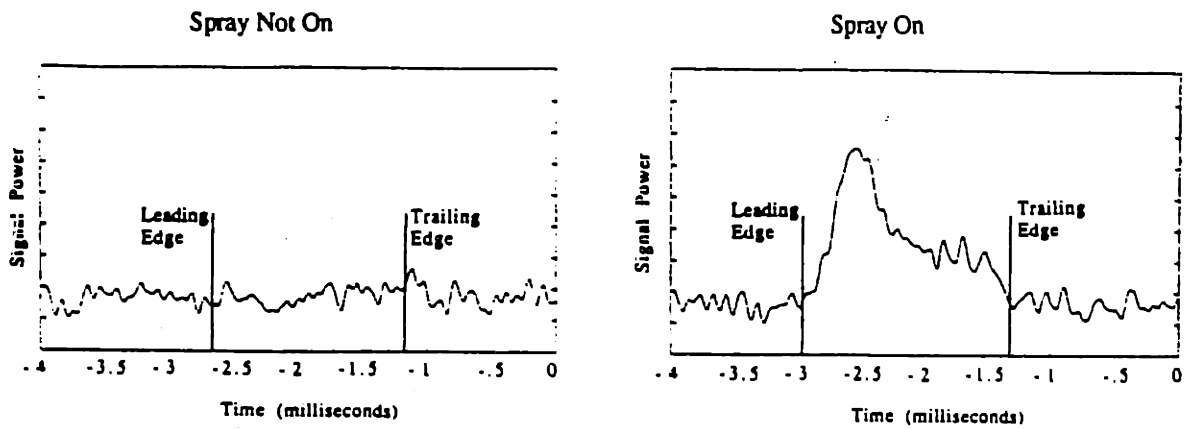


Fig. 14. IR Profiles at $T=-6.8^{\circ}\text{C}$ with and without water spray

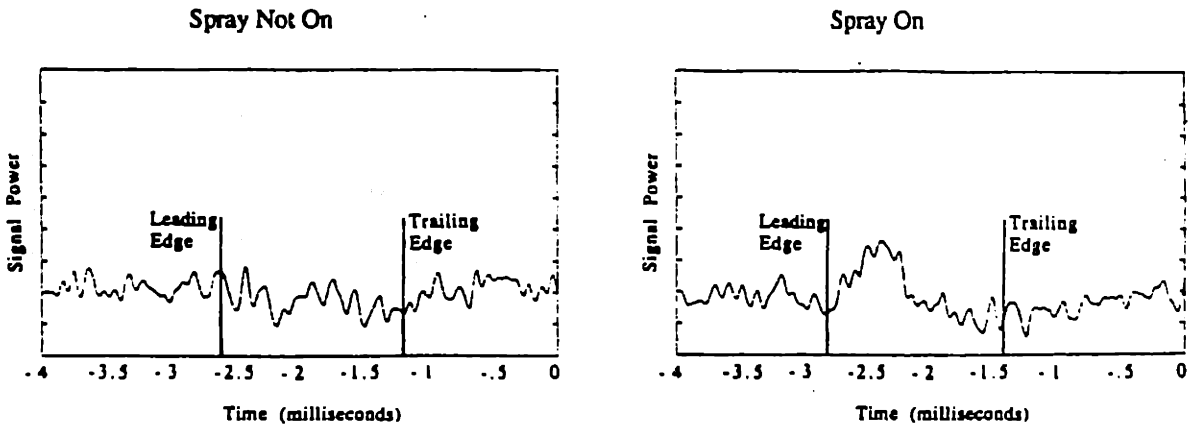


Fig. 15. IR Profiles at $T=-3^{\circ}\text{C}$ with and without water spray

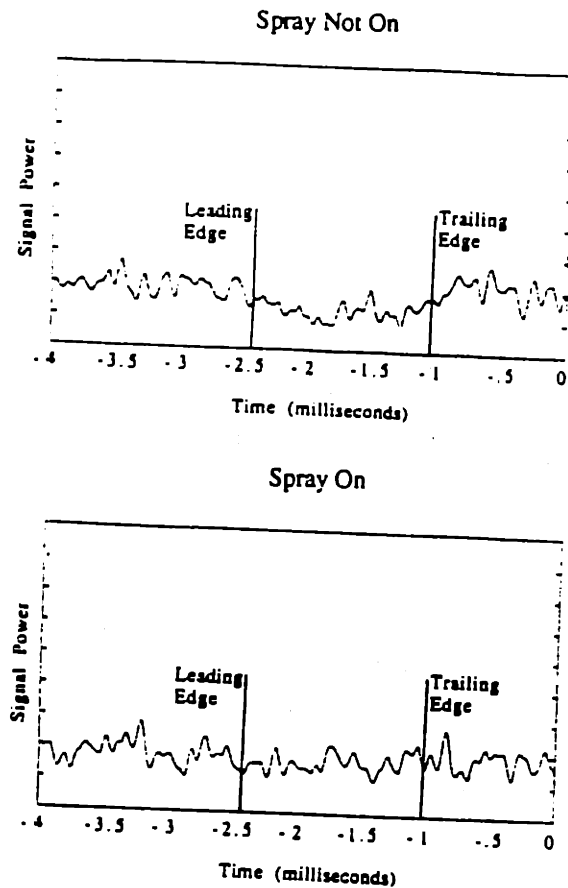


Fig. 16. IR Profiles at $T = -0.4^{\circ}\text{C}$ with and without water spray

4. Implementation Issues

While the above experiments indicate the potential of remote IR ice detection there are still several implementation issues to be considered. The rotor model did not include blade flapping or significant blade bending. These effects, in a helicopter application, will make it more difficult to track the blade location, and to keep it in focus. This may be addressed by use of a wide depth of field, or use of an auto focus system referenced to the blade leading edge.

Another issue to be considered is placement of the pyrometer on the helicopter. It will be necessary to mount the pyrometer so that it can view the blades, or possibly the tail rotor. Although small amounts of frost on the lens did not significantly degrade the signal in the rotor tests, it will be necessary to prevent the lens of the pyrometer from icing, frosting or becoming wet.

Signal processing is also an implementation issue, although it should be fairly straightforward. The signal must be amplified and synchronized with the rotor. It must be filtered, and then the profile compared to known icing conditions to determine the presence of ice. A simple leading edge to trailing edge temperature difference method may prove adequate. This data must be presented to the pilot in a useful format.

5. Conclusion

The results from preliminary IRT experiments, and the follow up rotor tests indicate that passive infrared ice detection can be used to remotely detect ice accretion on airfoils and rotors by measuring the characteristic chordwise temperature profiles which result from the release of latent heat during freezing. The technique has promise as a technique for remotely monitoring the icing of helicopter rotor blades. A prototype, suitable for flight testing, has been developed and successfully tested on a small scale rotor.

Acknowledgements

This work was supported by the National Aeronautics and Space Administration under grant NGC 3-927. The authors would like to thank the B.F. Goodrich Company and the Douglas Aircraft Company for their cooperation during the IRT tests and Professor Ken Dewitt and Alan Yaslick for providing thermocouple data.

References

1. Heinrich, A. Ross, R. Zumwalt, G., Provorse, J., and Padmanabhan, "Aircraft Icing Handbook - Vol. I", DOT/FAA/CT - 88/8-1, March 1988.
2. Corley-Byrne, P.L., "Helicopter Icing and It's Measurement". Presentation at SAE subcommittee meeting AC-9C - Aircraft Icing Technology, October 1986.
3. Hansman, R., Yamaguchi, K., Berkowitz, B., and Potapczuk, M., "Modelling of Surface Roughness Effects on Glaze Ice Accretion", AIAA-89-0734, AIAA 27th Aerospace Sciences Meeting, January 1989.
4. Henry, R. and Guffond, D., "Application de la Thermographie Infrarouge a l'Interpretation d'Essais dans une Soufflerie Givrante", Societe Francaise des Thermiciens, January 1989.
5. Skebe, S., "Synchronous Thermography", 3rd Japan-China joint conference on Fluid Machinery, April 1990